METAMORPHISM OF METABASITES FROM PARRY ISLAND, GEORGIAN BAY, ONTARIO.

Roberta Jean Hicks

Submitted in Partial Fulfilment of the Requirements
for the Degree of Bachelor of Science, Honours.
Dalhousie University, Halifax, Nova Scotia
March 1992

Distribution License

DalSpace requires agreement to this non-exclusive distribution license before your item can appear on DalSpace.

NON-EXCLUSIVE DISTRIBUTION LICENSE

You (the author(s) or copyright owner) grant to Dalhousie University the non-exclusive right to reproduce and distribute your submission worldwide in any medium.

You agree that Dalhousie University may, without changing the content, reformat the submission for the purpose of preservation.

You also agree that Dalhousie University may keep more than one copy of this submission for purposes of security, back-up and preservation.

You agree that the submission is your original work, and that you have the right to grant the rights contained in this license. You also agree that your submission does not, to the best of your knowledge, infringe upon anyone's copyright.

If the submission contains material for which you do not hold copyright, you agree that you have obtained the unrestricted permission of the copyright owner to grant Dalhousie University the rights required by this license, and that such third-party owned material is clearly identified and acknowledged within the text or content of the submission.

If the submission is based upon work that has been sponsored or supported by an agency or organization other than Dalhousie University, you assert that you have fulfilled any right of review or other obligations required by such contract or agreement.

Dalhousie University will clearly identify your name(s) as the author(s) or owner(s) of the submission, and will not make any alteration to the content of the files that you have submitted.

If you have questions regarding this license please contact the repository manager at dalspace@dal.ca.

Grant the distribution license by signing and dating below.

_____ _____

Name of signatory Date

ABSTRACT A garnet amphibolite body in the Parry Island shear zone, Central Gneiss Belt, Grenville Province, shows textural and mineralogical evidence of retrograde metamorphism to amphibolite facies. Garnets with plagioclase coronas, and clinopyroxene replaced by amphibole, illustrate the reaction Gnt + Cpx + H_2O = Plag + Hb, with the degree of reaction dependent upon deformation and fluid access. Petrological, compositional, and thermobarometric studies support the proposal that these rocks are retrograded from granulite facies. The least deformed sample best preserves relict textures and phases (relatively abundant clinopyroxene-plagioclase intergrowths associated with highly embayed garnets, and minor plagioclase corona development around less embayed garnets), and gives compositional evidence (An content in plagioclase, Al_2O_3/SiO_2, and Al^{IV} in amphiboles) of former higher temperatures. The same sample yields the highest pressure and temperature estimates. Another sample has amphiboles with pleochroism indicative of growth over a range of P-T conditions, and shows evidence that the most embayed garnets formed under higher pressure conditions. Textural similarities between the amphibolite and a meta-eclogite in the Britt domain suggest an earlier high-grade history for the amphibolite, however, evidence for an eclogite facies history is inconclusive. Temperature and pressure estimates average 650 °C and 6-7 kbars.

Key Words: Amphibolite, eclogite facies, geothermobarometry, granulite facies, Grenville Province, metamorphic history, retrogression.

TABLE OF CONTENTS

TABLE OF FIGURES

TABLE OF TABLES

ACKNOWLEDGEMENTS

I would like to thank Natasha Wodicka for her guidance and assistance both in the field and later, and Dr. Barrie Clarke for his invaluable criticism of the thesis at various stages in its development. Bob MacKay provided instruction and assistance with the microprobe work, and Gordon Brown prepared the thin sections.

I also want to thank the Parry Island Native Band Council for granting permission for field work on the Parry Island Reserve.

Melanie Haggart and Linda Richard gave invaluable assistance during the final stages. A special thanks to John Ketchum for valued support and hours of labour with computer programs, and to Bernice Moores for things too numerous to mention.

Finally, I wish to thank Dr. Becky Jamieson for all her guidance, support, and expertise while supervising this thesis.

CHAPTER 1 - INTRODUCTION

1.1 The Grenville Orogen

The Grenville Province is a 1.0 Ga orogenic belt extending from Georgian Bay in Ontario to eastern Labrador (Fig. 1.1). It is an example of a mid-to-deep crustal level orogen on the scale of large modern mountain systems (Culshaw et al. 1991). Several authors have suggested tectonic similarities to the Himalayas (Baer 1974; Davidson et al. 1982; Rivers et al. 1989), where crustal thickening exhumed high-grade metamorphic rocks of the orogenic belt. The Grenville orogen, unlike the Himalayas, has lost its upper crust through erosion (Wodicka 1990). As a result the Grenville Province is a well-exposed and valuable field laboratory for observing the products of processes that occurred at normally inaccessible depths.

Mountain belts experience a range of pressure and temperature conditions as they evolve through burial, uplift, and erosion. A knowledge of the geothermobarometry of high-grade metamorphic rocks, and the application of thermal models, contribute to our understanding of metamorphic processes at mid-to-deep crustal levels.

Portions of the Grenville Province have undergone one or more episodes of high-grade metamorphism (Wodicka 1990; Culshaw 1991; Davidson 1991; Jamieson et al. 1991). Separating the metamorphic history of the Grenville orogen from earlier metamorphic events is difficult. Studies of metamorphism and

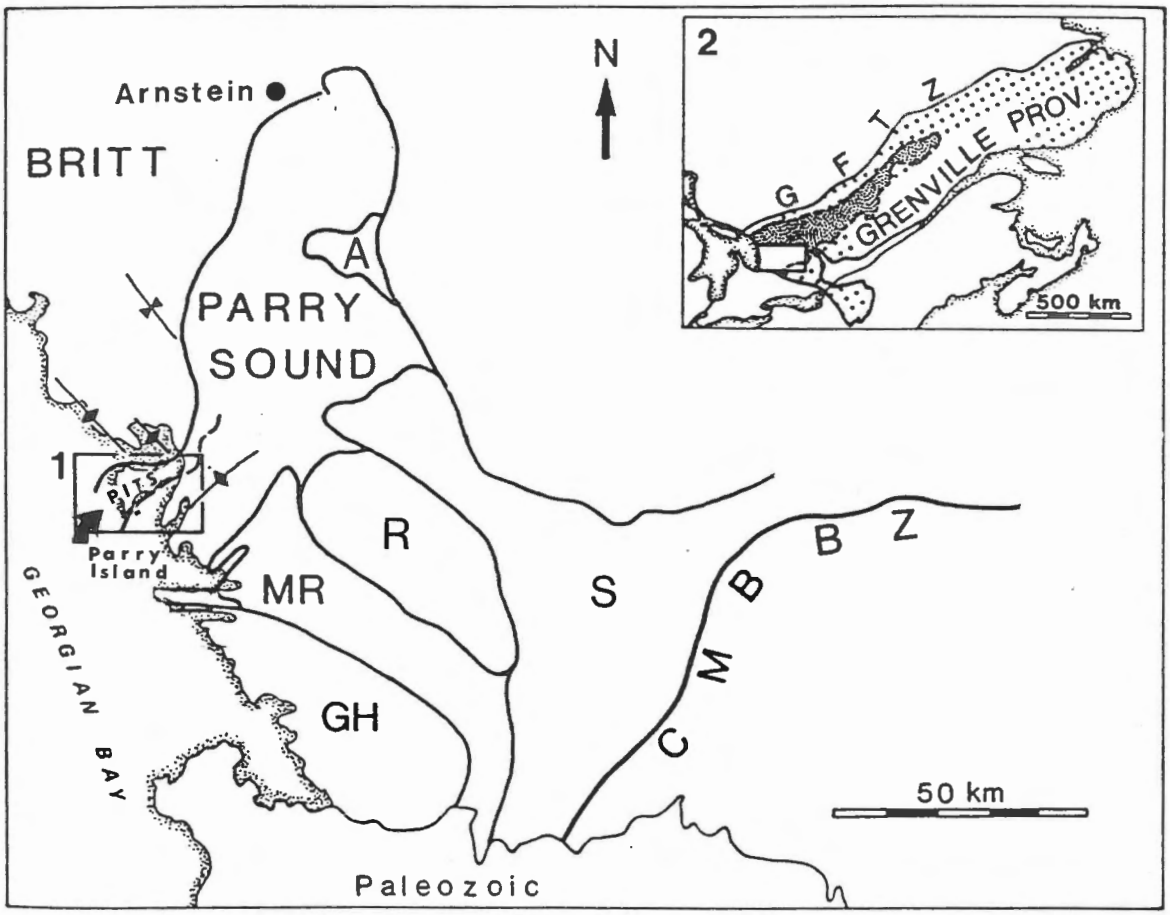

Fig. 1.1 Map showing the location of the study area (box 1) and structural divisions in the Central Gneiss Belt (after Davidson 1984). Britt and Parry Sound domains shown. **PITS** = Parry Island thrust sheet; **A** = Ahmic subdomain; **S** = Seguin subdomain; **R** = Rosseau subdomain; **MR** = Moon River subdomain; **GH** = Go Home subdomain; **CMBBZ** = Central Metasedimentary Belt Boundary Zone. Inset map (box 2) shows the location of the Central Gneiss Belt (fine stipple) within the Grenville Province (dots) (after Wynne-Edwards 1972). **GFTZ** = Grenville Front Tectonic Zone.

deformation in various units throughout the orogen are necessary to determine the tectonic history of the Grenville Province.

1.2 Metabasites in the Grenville Orogen

The Grenville Province has a variety of metamorphosed mafic suites, including the Sudbury dykes, coronitic metagabbros, amphibolites, and meta-eclogites, the last two commonly associated with anorthosite (Davidson 1990, 1991).

Metabasites are relatively competent rocks and, when subjected to high strain, they are more likely to retain former petrographic and chemical characteristics than neighbouring quartzo-feldspathic rocks. Metabasites can thus provide evidence of protolith type or previous, more intense, metamorphic events. Metamorphic assemblages, together with textural features, such as reaction coronas and replacement textures, can illuminate the metamorphic history of an area. Relict mineral phases can supply quantitative pressure and temperature information, depending on the timing of peak metamorphism. If mineral compositions have altered by diffusion during late-stage peak metamorphism, estimates of earlier P-T conditions are dubious.

Observed cross-cutting relationships may constrain the timing of metamorphic events, and mafic igneous rocks are particularly useful in this regard. Metabasites also serve as metamorphic markers that distinguish units having a similar appearance.

1.3 Parry Island Metabasites

A garnet amphibolite body located on the south shore of Parry Island, in the Parry Sound domain (PSD), Central Gneiss Belt, is an area of relatively low strain within a shear zone (Fig. 1.2). The metamorphic assemblages and relict textures present are well suited to a study of metamorphism and P-T conditions.

The Parry Sound domain comprises two units, the Parry Island thrust sheet (PITS) (Section 2.1 Regional Geology), and the interior Parry Sound domain (IPSD) (Wodicka 1990). The IPSD rocks have an early granulite-facies metamorphism, and some of the PITS rocks are interpreted as retrograded equivalents of the IPSD. The metamorphic grade of the PITS is generally upper amphibolite facies, but evidence exists of early granulite facies metamorphism in the amphibolite of the PITS (Wodicka 1990).

The amphibolite may also contain signs of eclogite facies metamorphism. Similarities in texture between the amphibolite and samples of a meta-eclogite from Arnstein (Fig. 1.1), within the central Britt shear zone (Davidson 1991), suggest the possibility of very high grade metamorphism for the PITS. Both the meta-eclogite and the amphibolite are located near thrusts and are associated with anorthosite bodies.

1.4 Objectives and Approach

This thesis examines a suite of garnet amphibolites and associated anorthositic gneisses from Armer Bay and Five Mile Bay

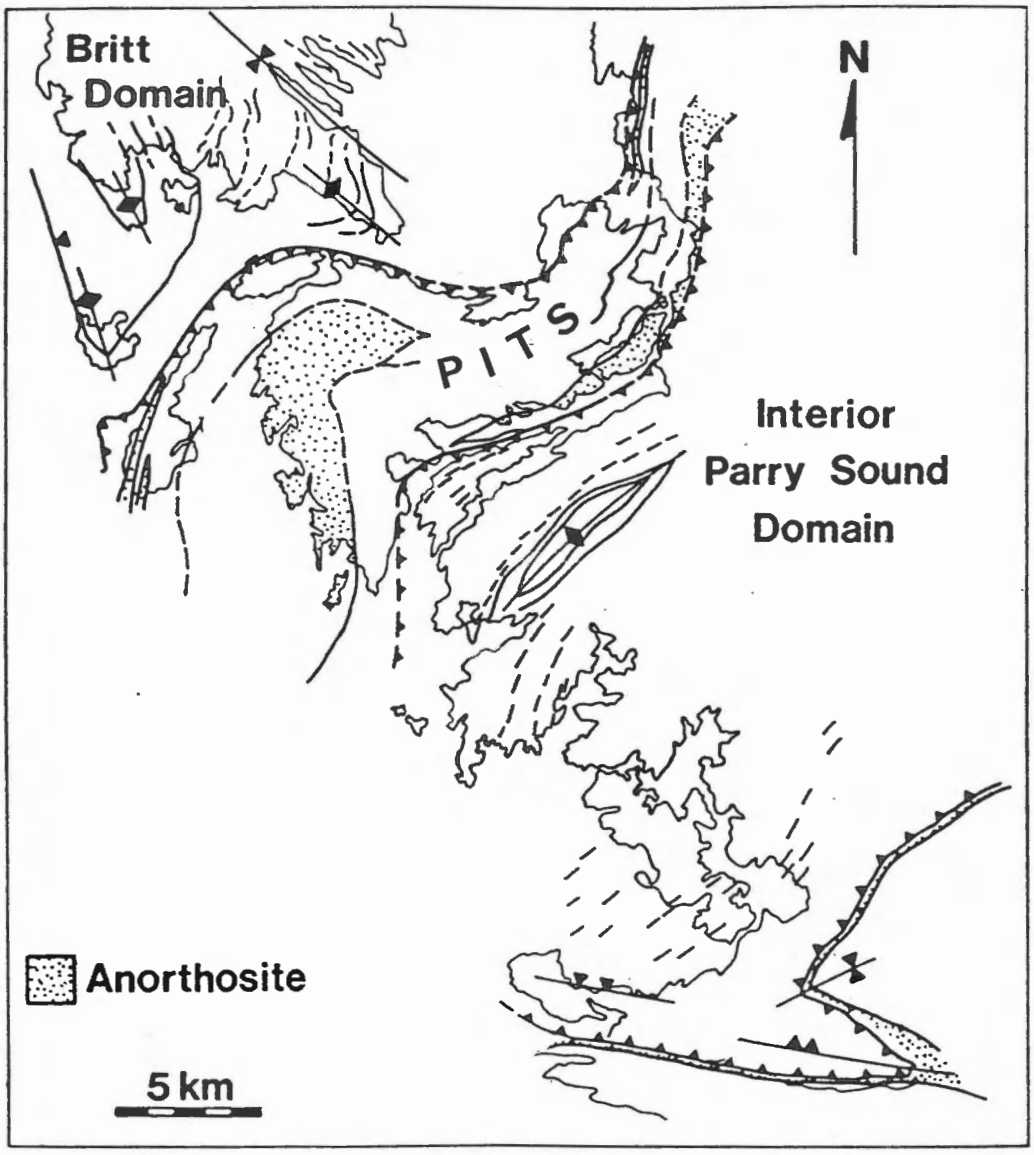

Fig.1.2 Geological sketch map of the Parry Island thrust sheet (PITS) and interior Parry Sound domain along Georgian Bay, showing structural relationships between different tectonic units (after Wodicka 1990).

on Parry Island (Fig. 1.3), and meta-eclogites from Arnstein. The amphibolites exhibit relict and replacement textures indicative of retrogression and decompression. The textural features, combined with pressure and temperature data, will help determine the metamorphic history of these rocks.

One of the goals of this study is to obtain pressure and temperature estimates indicative of the metamorphic history of the amphibolite. Another is to establish whether the PITS amphibolite had an early-granulite facies history, comparable to that of the IPSD. A careful examination of the phases and textures of the amphibolites and the meta-eclogite from Arnstein may show that the amphibolites experienced eclogite facies metamorphism.

Methods employed in this project include the following:

(i) detailed petrographic and microstructural studies of thin sections to provide data on metamorphic reactions and deformation;

(ii) chemical analyses obtained from electron microprobe studies to provide data for geothermobarometric calculations and for reconstructing phase relations; and

(iii) backscatter electron image analyses to examine details of textures and zoning.

1.5 Previous Work

The current phase of regional mapping of the Georgian Bay area of the Grenville Province began with the work of Davidson et

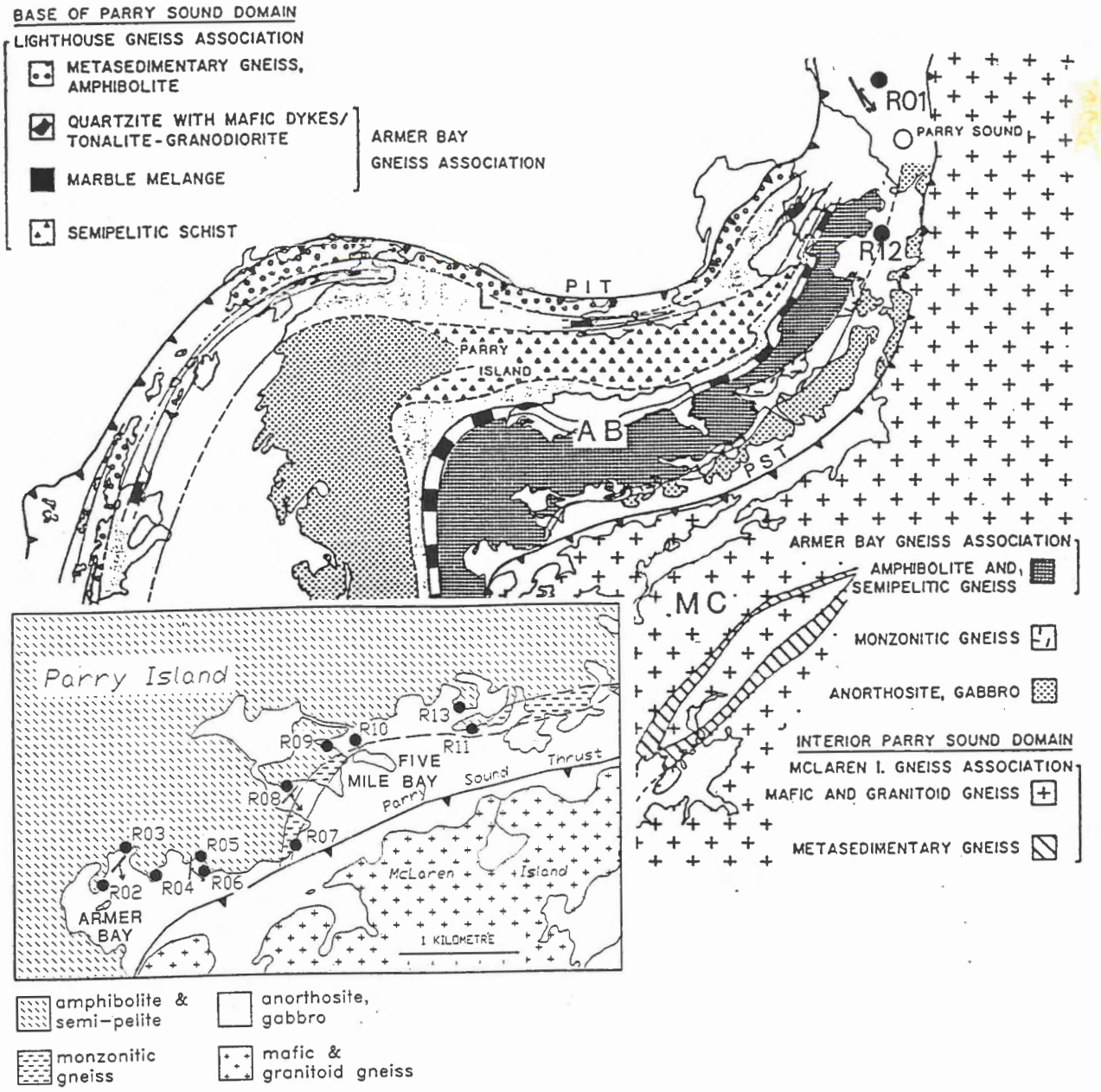

Fig.1.3 Geological map of the northern part of Parry Sound domain, Parry Island. Parry Island thrust **PIT** and Parry Sound thrust **PST** are indicated by barbed lines with barbs on upper plate. **L** = Lighthouse gneiss association; **AB** = Armer Bay gneiss association; **MC** = McLaren gneiss association (after Wodicka 1990). Inset map shows enlargement of thesis area. Numbered dots represent sample locations.

al. (1982), Culshaw et al. (1983, 1989, 1990), and Davidson and Bethune (1988). Although reconnaissance mapping is not complete, this area of the Grenville has been the subject of several detailed projects (Davidson 1984; Hanmer 1984; Nadeau 1984; Anovitz and Essene 1990; Ketchum in preparation; Wodicka in preparation). Most of these projects have addressed, or are addressing metamorphic (particularly thermobarometric) and structural problems. Geochronology studies of the southwestern Grenville Province are now in progress and will help constrain the early plutonic and metamorphic history of the area. Geochronological data for the area are summarized in Table 3.2.

1.6 Organization of the Thesis

This thesis first presents a regional geology overview with lithological, structural and field relations information for the field area. Petrography, and mineral chemistry data from electron microprobe analyses follow, and are the foundation for subsequent geothermobarometric studies. The discussion, and summary and conclusions, chapters synthesize the petrographic, mineral chemistry, and geobarometric data, and address the questions posed by this thesis.

CHAPTER 2 - REGIONAL GEOLOGY AND LOCATION

2.1 Regional Geology

Previous workers subdivided the Central Gneiss Belt of the southwestern Grenville Province into several lithotectonic domains and subdomains (Wynne-Edwards 1972; Davidson and Morgan 1981; Davidson et al. 1982; Culshaw et al. 1983; Davidson 1984; Davidson and Grant 1986) (Fig. 1.1). Their lithological, metamorphic, structural, and geophysical characteristics are distinct (Davidson 1991).

Culshaw et al. (1988, 1989, 1990a) describe smaller sub-divisions, called gneiss associations, that are also distinct and may have unique granitic plutons and mafic dykes. More recently, Culshaw et al. (1990b) recognized five tectonic units in the Central Gneiss Belt (Fig. 2.1), intermediate in size between (sub-)domain and gneiss association and exhibiting different lithologies and geologic histories.

Regional mapping has revealed northwest-directed thrusting illustrated by imbricate-style geometry. Domains and sub-domains are all separated by high-strain thrust surfaces with strong ductile deformation. Some boundaries between gneiss associations may represent cryptic thrust surfaces that have produced regional layering of units (Culshaw 1991).

Figure 2.1 shows the duplex style of structure suggested for the Central Gneiss Belt (Culshaw 1990b). Beneath the mid-crustal detachment are the polycyclic parautochthonous rocks of Unit 1.

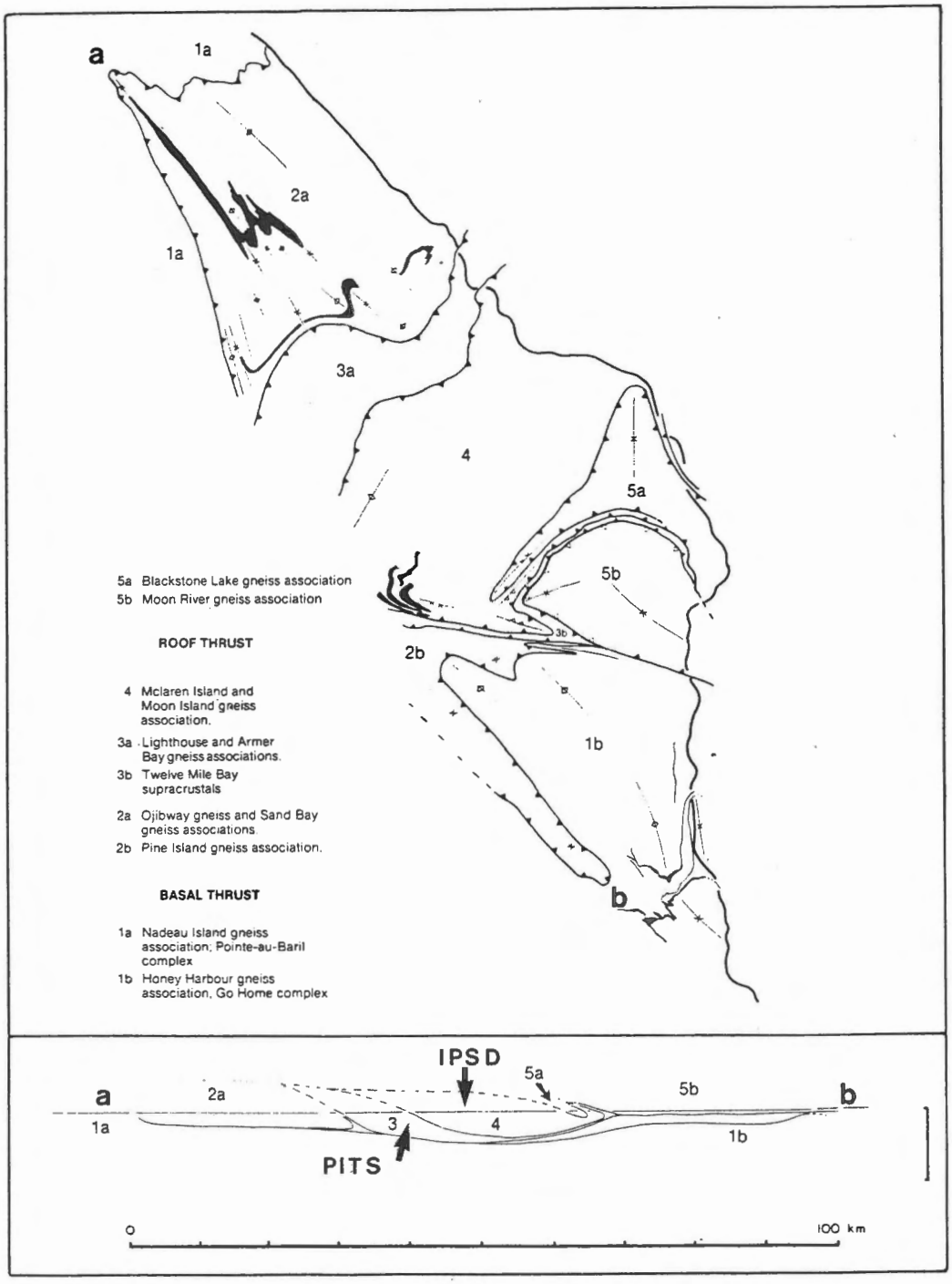

Fig.2.1 Tectonic outline of part of Georgian Bay transect. On map: teeth on upper plate of thrusts; on NW-SE cross-sections: solid lines = thrusts. Key: **1** = parautochthonous footwall; **2** to **4** = duplex units; **5** = roof; **3** = Parry Island thrust sheet (PITS); **4** = interior Parry Sound domain (IPSD) (after Culshaw et al. 1991).

Above are smaller allochthonous units including the Parry Sound domain (PSD) which comprises Units 3 and 4 (Culshaw 1990b; Wodicka 1990). The allochthonous terranes may be deeper levels of crust incorporated into the duplex structure, and their pre-thrusting metamorphic grade may have been granulite or eclogite facies. Later decompression and retrograde metamorphism resulted from the Grenvillian thrusting.

Parry Island, in the Central Gneiss Belt, is located on the northern boundary of the Parry Sound domain (PSD), where the PSD has thrust northwestward onto the Britt domain (Fig. 1.2). The PSD is divided into the interior Parry Sound domain (IPSD) and the Parry Sound shear zone (PSSZ) (Davidson 1984, Davidson et al 1982). However, the PSSZ has recently been interpreted as a distinct thrust sheet, renamed the Parry Island thrust sheet (PITS) (Wodicka, pers comm 1991). The northern boundary between the PSD and the Britt domain is now called the Parry Island thrust (PIT) and the tectonic break between the PITS and the IPSD is the Parry Sound thrust (PST) (Fig. 1.3) (Wodicka 1990). This thesis uses the newer terminology.

2.2 Location of the Study Area

Parry Island is located on Georgian Bay, midway along the eastern shore of Lake Huron, Ontario. Access is by way of Highway 69 to the town of Parry Sound and by bridge to the island itself.Field mapping in the area is easiest by boat as shoreline

outcrops are well exposed. The Parry Island Indian Band Council generously granted permission to work on the island.

Figure 1.3 shows sample locations along Armer Bay and Five Mile Bay on the southern shoreline of Parry Island. Sample R12 is from Rosetta Island off the east coast of Parry Island in the harbour. Other samples are from location R01 at the intersection of Highways 69 and 69B, and from Arnstein (Fig. 1.1). Field work was carried out by boat and vehicle in June and August of 1990.

CHAPTER 3 - LITHOLOGIES, STRUCTURE, AND FIELD RELATIONS

3.1 Lithologies

The Parry Island thrust sheet (PITS) consists of upper amphibolite facies supracrustal rocks with subordinate metaplutonic rocks and discrete bodies of anorthosite (Fig. 1.3, Table 3.1). These comprise the Lighthouse and Armer Bay gneiss associations which overthrust the migmatitic gneisses of the Britt domain to the north. The metaplutonic granulites (granitoid orthogneisses and mafic gneisses) of the McLaren Island gneiss association (IPSD) overthrust the PITS (Wodicka 1990, Culshaw 1991).

The Lighthouse and Armer Bay gneiss associations have different proportions of similar lithologies. The supracrustal rocks include pelites, semi-pelites, psammites, metaquartzites, calc-silicates, amphibolites, and marbles. Gabbroic anorthosite, tonalite, granodiorite, and monzonite are also present. Mafic dykes cut quartzite, anorthosite, and tonalitic-to-granodioritic orthogneisses, and are themselves metamorphosed and deformed (Wodicka 1990).

The thesis area lies within the Armer Bay gneiss association: garnet amphibolite with interlayered migmatitic feldspathic paragneisses, monzonitic gneisses, and rare pelitic gneisses and quartzites (Culshaw 1991). A variety of sizes of gabbroic anorthosite bodies are present, including the southward extending tail of the Whitestone pluton (Nadeau 1984). The

Table 3.1 Summary of Lithological Units, Parry Sound Domain. Unit numbers as shown in Figure 2.1.

Unit 4 - Interior Parry Sound domain (IPSD)	
McLaren Island gneiss association	Metaplutonic granulites (1425 ± 75 Ma): interlayered mafic gneiss and granitoid orthogneiss, minor (semi-) pelitic gneiss and marble, mafic dykes.
Moon Island gneiss association	Metaplutonic rocks: quartz diorite, diorite, charnockite, mafic gneiss, minor supracrustal rocks.
Metamorphism	Granulite facies (Opx + Sill) (1161 ± 3 Ma), locally retrogressed to amphibolite.
Unit 3	
3a Parry Island thrust sheet (PITS)	Amphibolite, (semi-) pelitic gneiss and schist, quartzite (≤ 1360 Ma), tonalitic to granodioritic orthogneiss with mafic dykes, (Quartzo-) feldspathic gneiss, minor marble. Anorthosite-gabbro; Parry Island anorthosite (1163 ± 3 Ma) and Whitestone anorthosites (ca. 1350 ± 50 Ma, van Breemen et al. 1986), slivers and isolated boudins of anorthositic gneiss. Late syntectonic pegmatite (1158 ± 2 Ma), aplite (1158 ± 1 Ma). Monzonite orthogneiss.
Lighthouse and Armer Bay gneiss associations, and **3b Twelve Mile Bay supracrustals**	
Metamorphism	Relict Opx in dykes, metaplutonic rocks (≤ 1350 Ma). Upper amphibolite facies pelites Ky-Sill-Staur (ca. 1120 Ma).

(After Jamieson et al. 1991; Wodicka 1990, 1991 pers comm.).

Table 3.2 Timing of Thrusting and Metamorphism in Parry Sound Domain

U-Pb age (Ma)	Event	Reference cited
1161 ± 3 (z)	granulite facies metamorphism, IPSD	van Breeman et al. (1986)
1159+5/-4 (z)	early thrusting of IPSD over PITS	van Breeman et al. (1986)
>1149 ± 3 (z)	metamorphic age from amphibolite, PITS	Wodicka & Parrish, unpublished data
1121 ± 5 (z)	late thrusting of IPSD over PITS	van Breeman et al. (1986)
1116+16/-10 (m)	upper amphibolite facies metamorphism, PITS	Wodicka & Parrish, unpublished data
1090 ± 20 1078 ± 2 1077 ± 2 (t)	titanite cooling ages PITS	Wodicka & Parrish unpublished data

z = zircon
m = monazite
t = titanite

anorthosite is strongly mylonitized in places and closely associated with granodioritic to monzonitic orthogneiss.

3.2 Structure

The Parry Island thrust sheet (PITS) is a southeast-dipping ductile shear zone interpreted as a major tectonic boundary separating the northern Parautochthonous Belt and allochthonous terranes to the south (Fig. 2.1) (Rivers et al. 1989). The sequence of thrusting began with the interior Parry Sound domain (IPSD) thrusting northwestward over the PITS. Both units then overthrust the Britt domain in the same direction (Davidson and Morgan 1981; Davidson et al. 1982; Davidson 1984, 1986; Nadeau 1984).

Throughout the PITS, structures at the macroscopic and microscopic scale demonstrate the effects of intense ductile deformation. Foliation strikes northeastward to eastward with gentle to moderate dips while a pervasive lineation plunges to the southeast. Axes of tight to isoclinal folds and tube axes of sheath folds are always parallel and subparallel to the lineation (Wodicka 1990) (Fig. 3.1).

On Parry Island and on the highway at Parry Sound, foliation measurements are consistent with known regional trends. Lineation measurements approximate the southeastward plunging regional lineations typical of the PITS (Fig. 1.3).

Shearing and deformation have produced a subequigranular granoblastic texture in the straight gneisses, and extensive

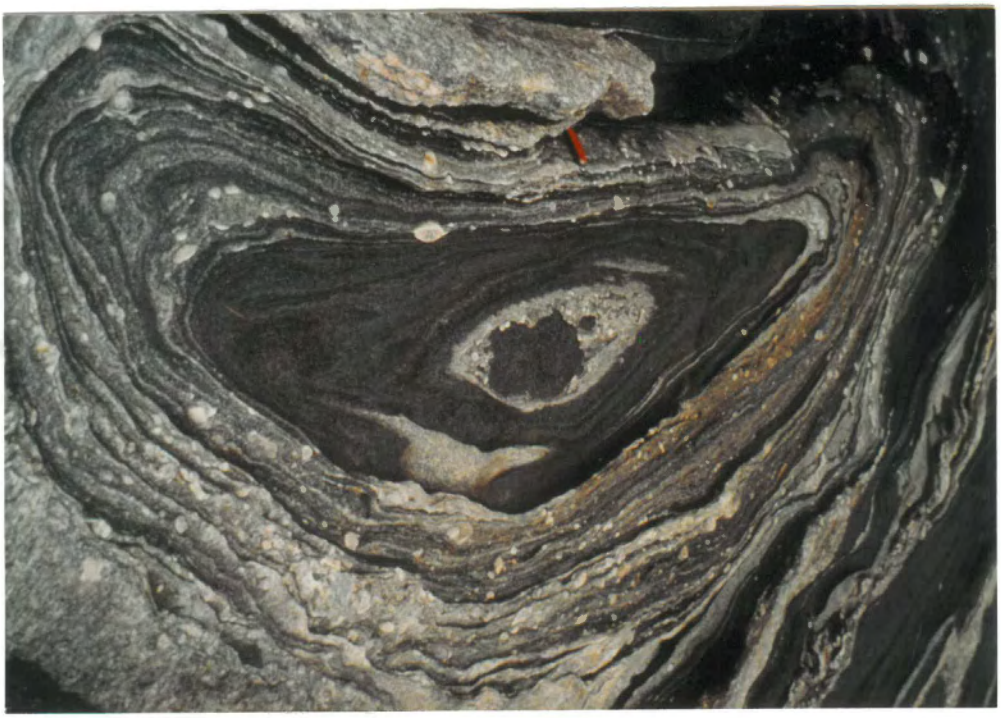

Fig. 3.1 Sheath fold in porphyroclastic gneiss. Pocket knife oriented parallel to stretching lineation (Wodicka 1990).

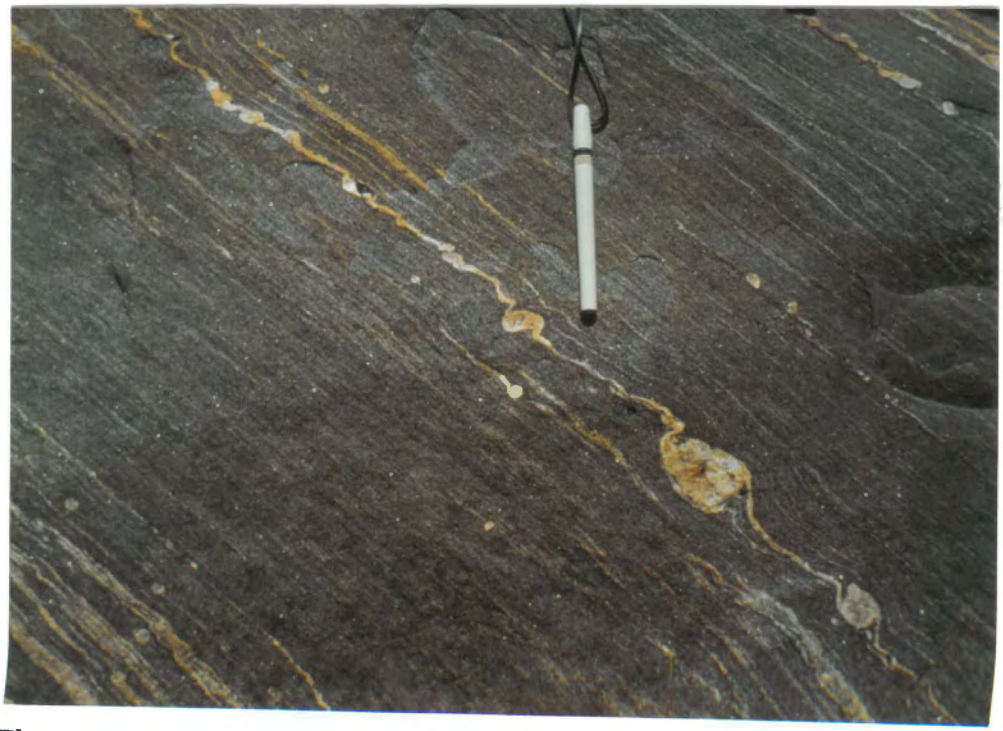

Fig. 3.2 Three rotated K-feldspars (delta) in mafic gneiss, with thrusting sense toward NW (Wodicka 1990).

grain size reduction in the feldspathic and quartzofeldspathic mylonites and protomylonites (Wodicka 1990). As well, strain is evident in deformed porphyroblasts (Section 3.3 - Field Relations).

Kinematic indicators reflect the northward-directed regional thrusting direction (Fig. 3.2).

3.3 Field Relations

All samples come from the Armer Bay gneiss association, except for the samples of meta-eclogite from Arnstein. The Armer Bay lithology is predominantly garnet amphibolite and anorthosite. Garnet amphibolite samples contain garnet porphyroblasts with plagioclase coronas. Although the garnet cores show no sign of strain, the plagioclase rims extend parallel to the lineation direction (Fig. 3.3).

Some amphibolites are massive while others are layered. In outcrops where both varieties are present, the contact between the two is gradational (Fig. 3.4). Outcrop R01 has an anastomosing fabric around pods of less deformed amphibolite. These pods show a lineation that is not parallel to the general lineation, and the porphyroblasts display no deformation.

Hornblende-garnet anorthosites are associated with the amphibolites (sample sites R07, R09, R10, R11). Contacts between amphibolites and anorthosites are usually cryptic, but are sheared in one outcrop (Fig. 3.5).

Fig. 3.3 Mafic gneiss. Plagioclase partially rimming garnet is stretched parallel to lineation (Wodicka 1990).

Fig. 3.4 Gradational contact between massive and layered garnet amphibolite. Sample R04, Armer Bay.

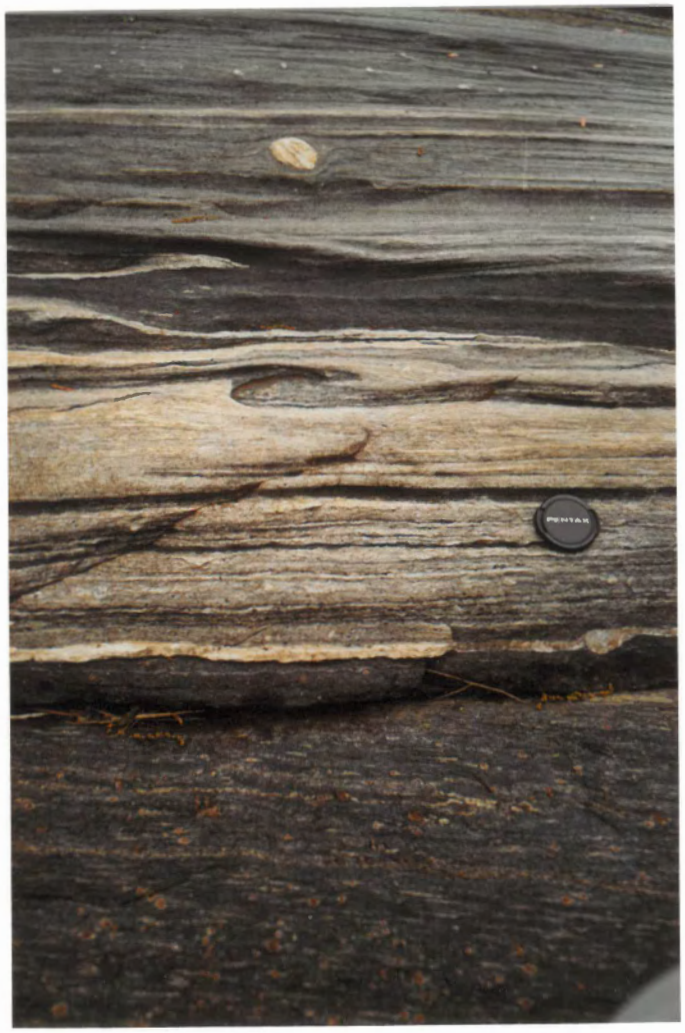

Fig. 3.5 Sheared contact between anorthosite (top) and garnet amphibolite (bottom). Note difference in strain between rock types. Sample R07a, Five Mile Bay.

Other rock types present in the study area include quartzo-feldspathic gneiss, often in layers (sometimes migmatized) within the amphibolite. Minor calc-silicate pods associated with the contact between the amphibolite and the quartzo-feldspathic gneiss are less common. A succession, bottom to top, of metasediments, layered amphibolite, massive amphibolite, and quartzo-feldspathic gneiss exists at outcrop R06. Minor metasediments, including possible quartzite, are present at one location. The nature of the contacts between the metasediments, quartzite, and amphibolite is unknown.

Monzogranite at sample sites R09 and R10 appears to have intruded the anorthosite. Inclusions of anorthosite also occur within the monzogranite at outcrop R10; contacts are sharp and sheared, but the anorthosite underlies the known anorthosite-monzogranite contact. At this location there is also a gabbroic intrusion into the anorthosite. At location R08 a grey mylonite mixed with amphibolite bounds the amphibolite on both sides. The amphibolite shows markedly less strain than the mylonite. A mylonitized orthogneiss is present with the layered amphibolite at outcrop R13.

Leucosomes, predominantly feldspar with some quartz, have formed in many outcrops. They display both sharp and diffuse contacts with more mafic portions of the rocks. Clinopyroxene is present in many of the amphibolites, usually in the leucosomes (Fig. 3.6). Some samples (R09, R12, R13) have clinopyroxene in the more mafic areas of the amphibolite. Rotated plagioclase

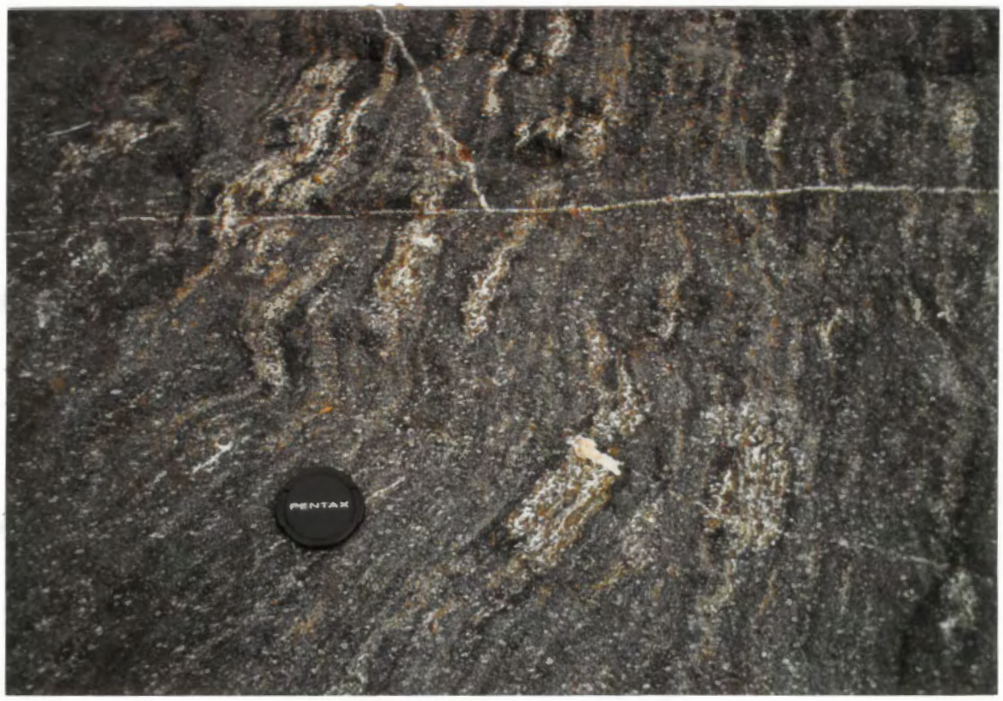

Fig. 3.6 Layered garnet amphibolite. Close-up showing leucocratic layering with clinopyroxene. Sample R04, Armer Bay.

porphyroblasts (some with garnet cores) from several locations are consistently sinistral (Fig. 3.2), agreeing with the regional northwestward direction of thrusting. Pegmatites cut the fabric, and are straight, or deformed to varying degrees. Quartz veins are also common, usually less deformed than the pegmatites and, in one outcrop, resemble tension gashes.

More detailed studies of the lithologies in Chapter 4 will focus mainly on the Parry Island garnet amphibolite and meta-eclogite from Arnstein, with less emphasis on the anorthosite. Selected amphibolite samples include those demonstrating the least retrogression and strain (containing abundant clinopyroxene and garnet with the least plagioclase corona growth), but samples exhibiting more strain and retrogression are also significant for subsequent petrography.

CHAPTER 4 - PETROGRAPHY AND MINERAL CHEMISTRY

4.1 Introduction

Twenty-four samples from the Parry Island and Arnstein locations form the basis of petrographic and mineral chemistry studies - 24 normal thin sections for routine petrography, and 7 polished sections for subsequent electron microprobe work. The purpose of the petrographic study is to examine the metamorphic phases and textural relationships present in the samples. Microprobe analyses are from core-to-rim traverses of between two and six garnet grains per thin section. Garnet traverses range from three to eight points, depending on the size of the porphyroblast. Analyses of matrix and corona plagioclase grains are based on both core-to-rim traverses and single spot analyses of between two and eight grains per section. Both core-to-rim and single spot analyses from hornblende, clinopyroxene, and biotite grains come from two to six grains per sample (one to four grains per sample for boitite). Appendix I contains full petrographic descriptions of the thin sections.

4.2 Metamorphic Assemblages, Textures, and Chemical Compositions

In conjunction with a petrogenetic grid, metamorphic assemblages yield estimates of the pressure and temperature conditions of metamorphism. The textural relationships between the metamorphic minerals and the fabric can reveal the relative timing of metamorphism and deformation, and the overprinting sequence of different assemblages. Mineral chemistry provides

another level of information on relationships and reactions in these samples. Table 4.1 summarizes and compares mineral chemistry data for the sections probed. Complete chemical analyses of minerals are in Appendices IIa and IIb.

4.2.1. Garnet Amphibolite

Essential metamorphic minerals include garnet, plagioclase feldspar, hornblende, and clinopyroxene, with accessory titanite, opaque minerals (ilmenite?), biotite, quartz, carbonate, and scapolite. Muscovite, epidote, apatite, and chlorite are rare.

The stable phases are plagioclase, hornblende, biotite, titanite, and opaque minerals. Plagioclase is present in the matrix, as an intergrowth with clinopyroxene, and as coronas around garnet porphyroblasts (Fig. 4.1). Plagioclase composition is uniform within thin sections but varies considerably between samples. Thin sections R01f and R07a have An_{30-36} and An_{41-50} respectively, and section R13 has An_{75}. There is very little compositional difference between cores and rims, or matrix and corona plagioclase. This implies chemical equilibrium in plagioclase, which is supported by the presence of granoblastic plagioclase in coronas, and commonly in the matrix.

Amphibole, predominantly ferroan pargasitic hornblende and edenitic hornblende, has extensively replaced clinopyroxene. Amphibole classification is based on IMA guidelines (Leake and Winchell 1978,) as determined by AMPHIBOL software recalculation

Table 4.1 Summary of Mineral Compositions

Garnets	Almandine	Pyrope	Grossular
Amphibolite			
R01f	54-56	12-18	20-27
R07a	49-52	10-17	29-34
R13	50	43-74	39-44
Meta-Eclogite	36-44	30-41	20-25

Clinopyroxene	Wo	En	Fs	Jd
Amphibolite				
R01f	46	36	13-16	1-2
R07a	46	36-39	8-10	0-2
R13	45-47	28-30	17-19	1-3
Meta-Eclogite	42-44	42-43	5-7	3-4

	Amphibole Fe/(Mg+Fe)	Plagioclase An Content	Biotite Fe/(Fe+Mg)
Amphibolite			
R01f	0.41-0.48 and 0.38	30-36	
R07a	0.46-0.48	41-50	
R13	0.62-0.65	75	
Meta-Eclogite	0.24-0.31	28-44	0.27-0.28
Anorthosite	0.62-0.68	30	0.55-0.57

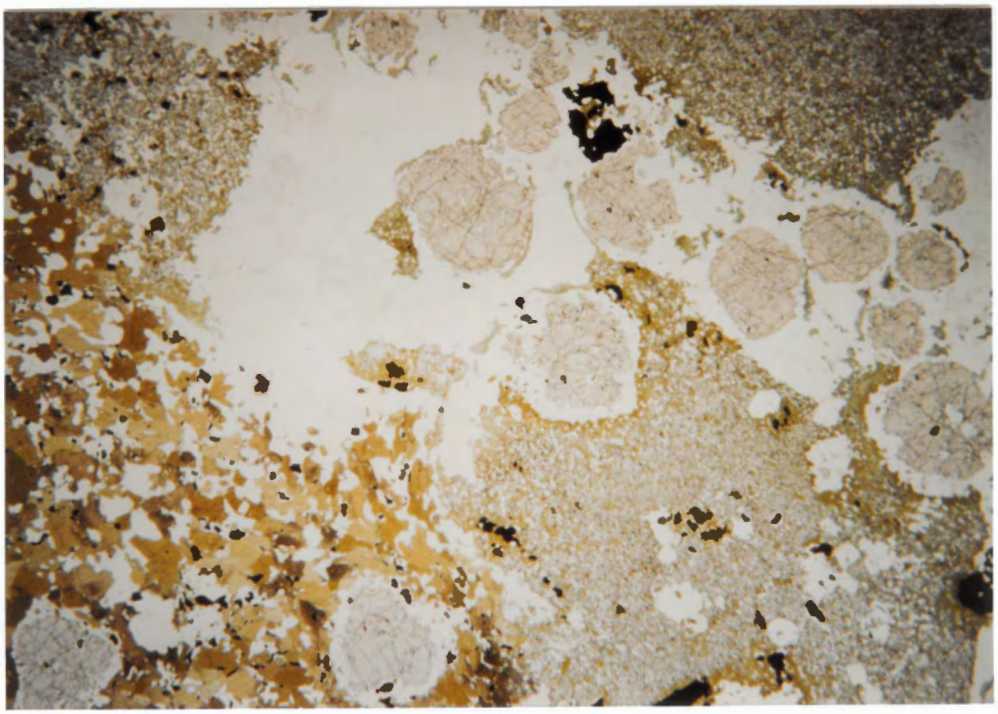

Fig. 4.1 Garnet amphibolite showing clinopyroxene-plagioclase intergrowth (right), hornblende replacing clinopyroxene (left), and garnet rimmed by plagioclase. Sample R01f, Parry Sound. 1.0 x 0.5 cm.

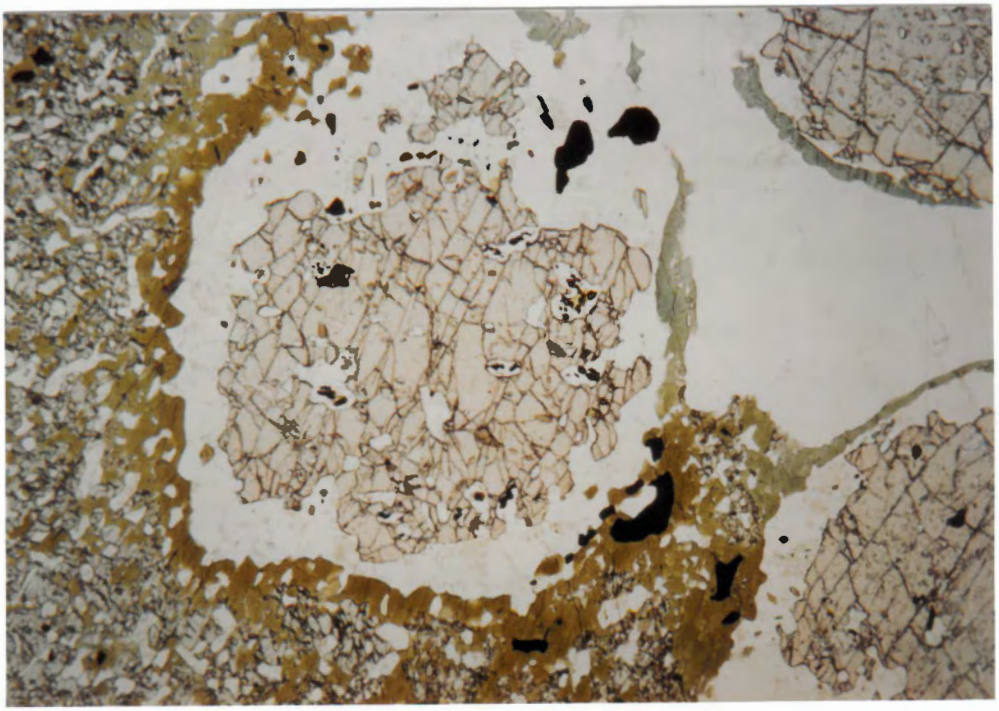

Fig. 4.2 Embayed garnet with plagioclase corona. Hornblende replacing clinopyroxene-plagioclase intergrowth. Two colours of amphibole visible. Sample R01f, Parry Sound. 4 x 6 mm.

(Richard and Clarke 1990). Amphiboles have a variable Fe/(Mg+Fe) ratio of 0.38 to 0.65. Within individual thin sections the range is smaller (R07a: 0.46-0.48, R13: 0.62-0.65), but sample R01f has a range of 0.41 to 0.48 and one anomalous value of 0.38. Variable concentrations of Al_2O_3 reflect the presence of several types of amphibole including edenitic hornblende, magnesio-hornblende, actinolitic hornblende, and ferroan hornblende. Locally, hornblende texture mimics that of the clinopyroxene intergrowth it is replacing, but (sub)idioblastic grains are also present. Two distinct colours of amphibole are visible microscopically; the light green is edenitic hornblende and the dark green grains are magnesio-hornblende and ferroan hornblende. The pleochroic scheme of hornblende varies with metamorphic grade, becoming generally darker at higher grade, probably owing to increasing Ti relative to Fe (Raase 1972). In sample R01f the two colours suggest hornblende growth at differing metamorphic conditions, with light green hornblende growth taking place near garnets and within plagioclase coronas (Fig. 4.2).

Biotite is a relatively late phase overprinting hornblende or, less commonly, plagioclase and garnet, often where there are quartz veinlets. No mineral chemistry is available for these biotites. Titanite is nearly ubiquitous as sub(idioblastic) grains with opaque (ilmenite?) cores, and is generally associated with mafic phases. The presence of scapolite is unusual in metabasites and suggests the involvement of CO_2-rich fluids. Scapolite is indicative of granulite facies conditions in other

rock types (i.e. anorthosite), but more basic scapolite-bearing lithologies such as amphibolites have been studied. Moecher and Essene (1990) discuss the possible role of CO_2 in granulite genesis (CO_2 flooding dilutes H_2O and produces a 'dry' metamorphism) and use the meionite content in scapolite to constrain the role of CO_2 in the formation of granulites. They note the presence of scapolite-bearing granulite facies amphibolites in several localities. O'Beirne-Ryan et al. (1989) use the meionite content in scapolite from garnet-clinopyroxene amphibolites in Mont Albert, Quebec to indicate upper-amphibolite to lower-granulite facies metamorphism in these rocks.

Garnet porphyroblasts and clinopyroxene both display disequilibrium characteristics. Garnet ranges from large (4 mm), sub-idioblastic grains with relatively minor fracturing and embayment, to disaggregated remnants (Fig. 4.3), to medium-sized, nearly idioblastic, apparently pristine grains (Fig. 4.4).

Garnets in these amphibolites are relatively almandine-rich and pyrope-poor compared with meta-eclogite (R01f: Alm_{54-56}, Pyr_{12-18}, and $Gros_{20-27}$; R07a: Alm_{49-52}, Pyr_{10-17}, and $Gross_{29-34}$; R13: Alm_{50}, Pyr_{43-74}, and $Gross_{39-44}$).

Garnets exhibit irregular fluctuations in compositional zoning (Figures 4.5 a & b). Normal growth zoning in garnets is usually characterized by bell-shaped Mn zoning and core to rim increases in Mg (Tracy 1982). Spot 6 garnet in sample R01F and the 'old' garnet in R07a have normal zoning profiles.

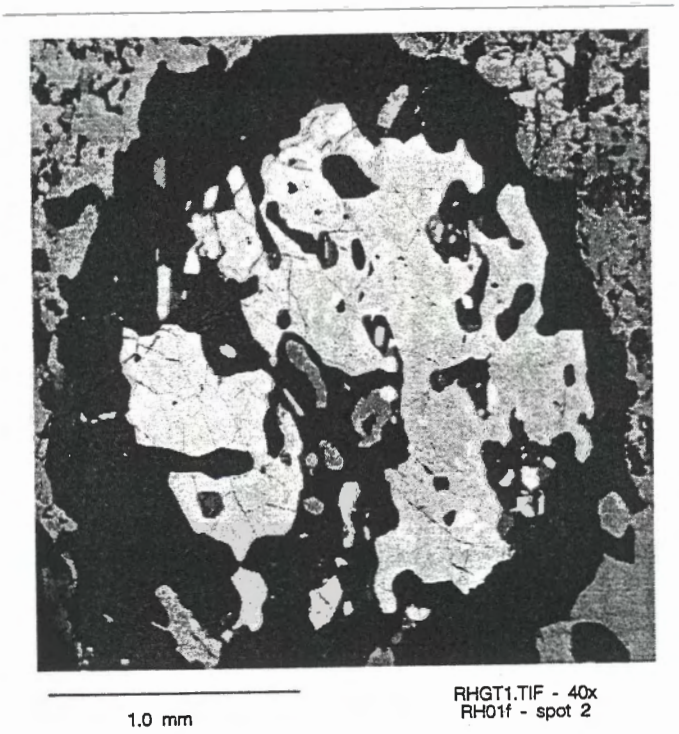

Fig 4.3 Backscatter electron image of embayed garnet with plagioclase corona. Sample R01f, Parry Sound.

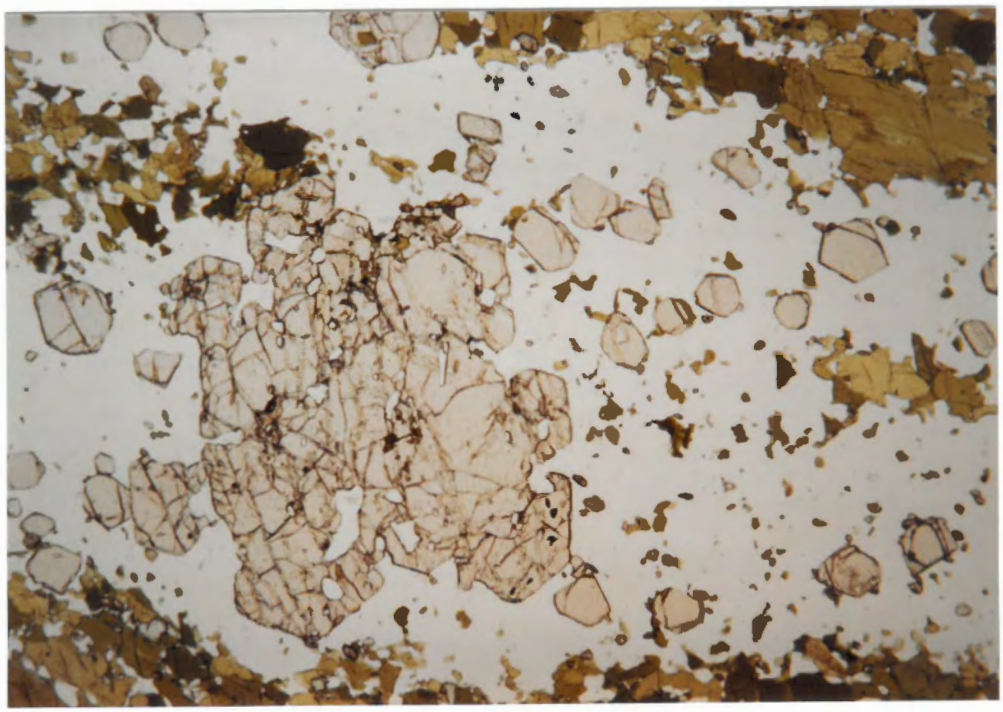

Fig. 4.4 Large, embayed, garnet porphyroblast with second generation of small, pristine garnets. Surrounded by deformed plagioclase corona. Sample R07a Five Mile Bay. 4 x 6 mm.

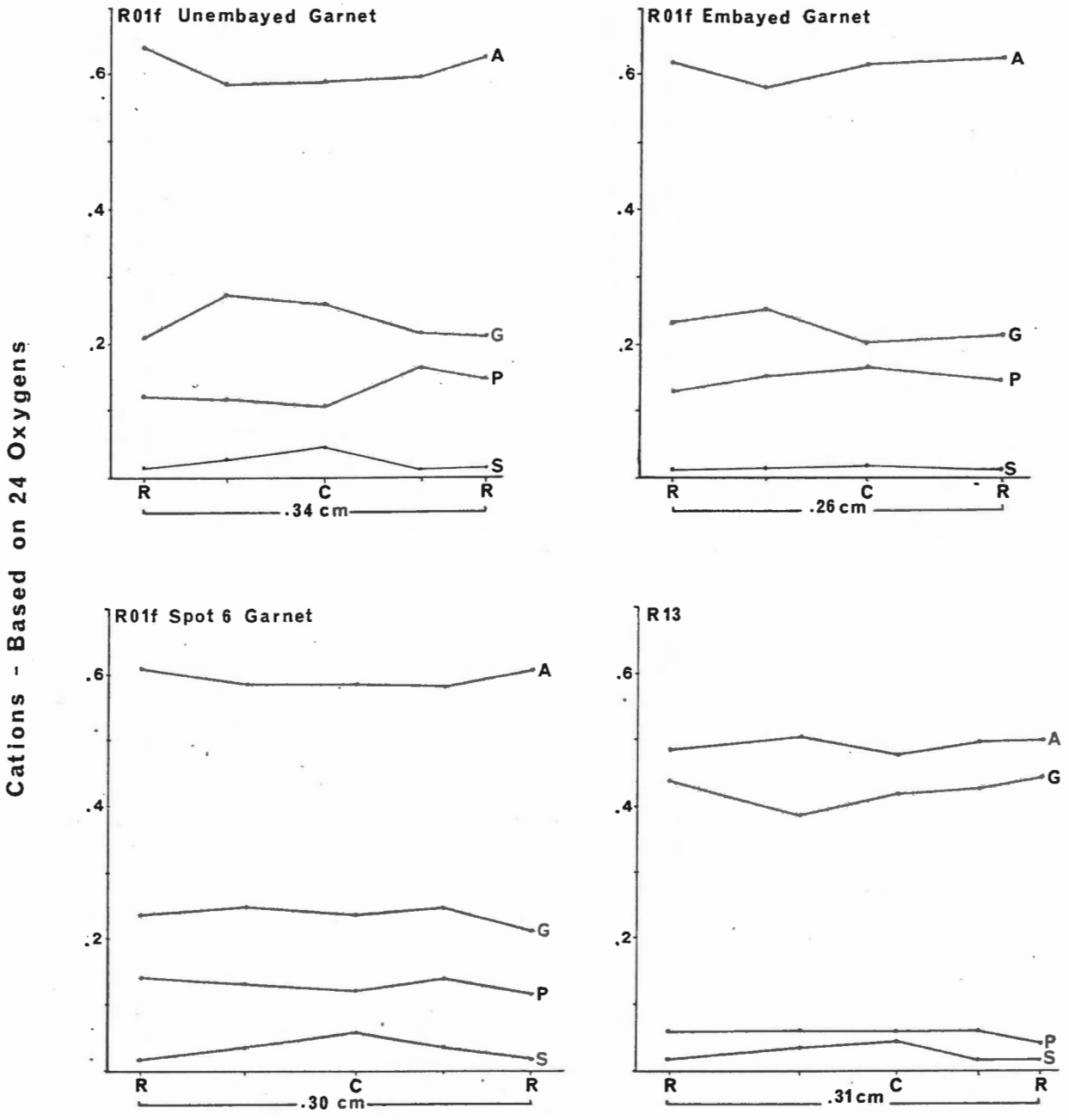

Fig. 4.5a Compositions vs distance plots of garnets in amphibolite showing zoning patterns for almandine, grossular, pyrope, and spessartine.

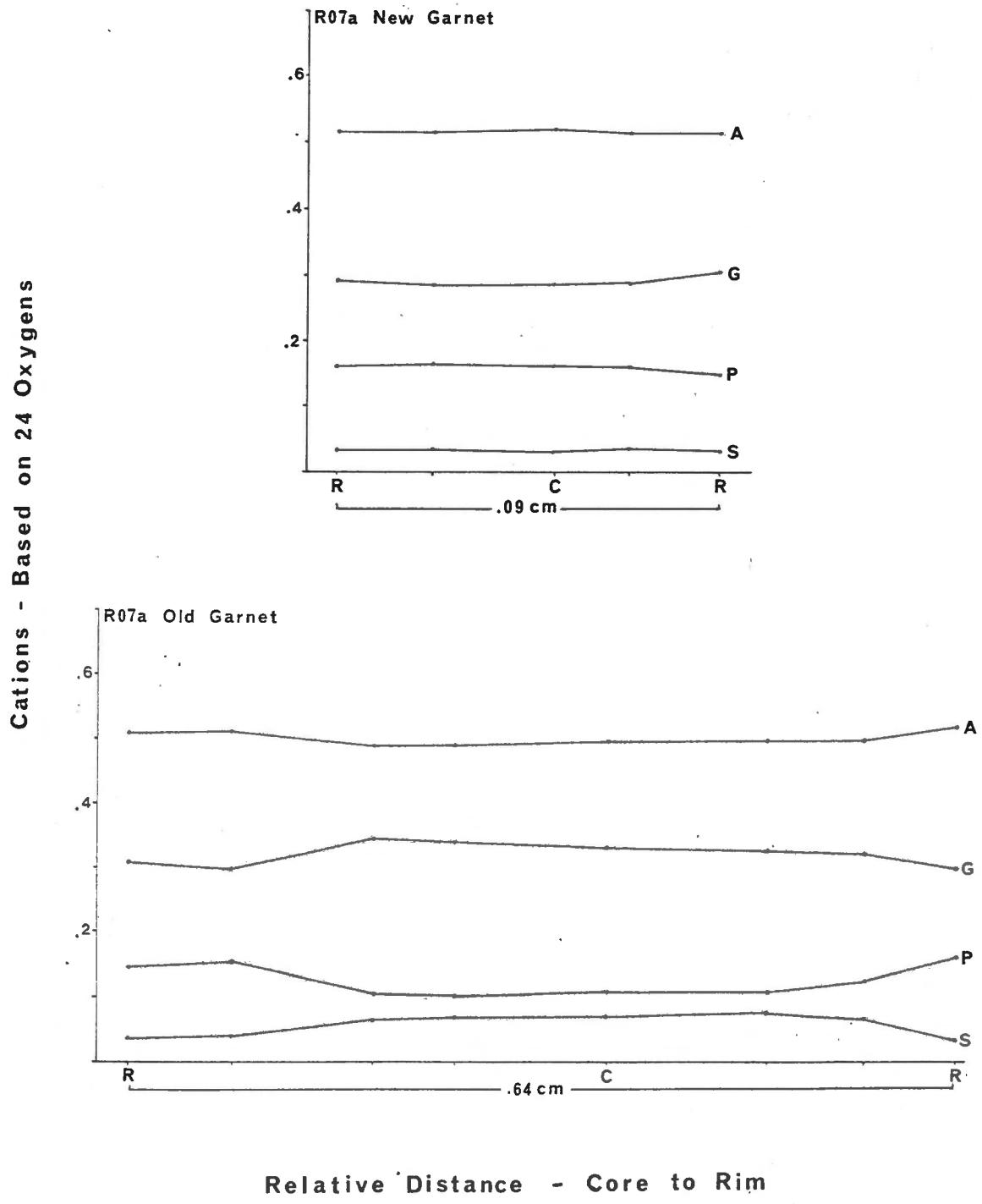

Fig. 4.5b Compositions vs distance plots of garnets in amphibolite showing zoning patterns for almandine, grossular, pyrope, and spessartine.

In contrast, the zoning profiles of garnets that have undergone homogenization followed by retrograde zoning include a core to rim increase in Mn, a decrease in Mg, and a flat Ca profile (Tuccillo et al. 1990). This type of zoning does not appear to be particularly characteristic of Parry Island garnets, although the embayed garnet from R01f, the 'new' garnet from R07a, and sample R13 do show a core-to-rim decrease in Mg.

The irregularities in these profiles result from variable degrees of re-equilibration with inclusions, and any pressure and temperature interpretations must take these variations into account. This is particularly true of sample R01f because it displays such variation. One of the garnets (spot 6) has a profile typical of retrograde zoning. Pressure and temperature data from this and other similar garnets probably give the most reliable estimates for this sample. All garnets have flattened zoning profiles, indicative of homogenization at a temperature of ~650 °C.

Garnets from sample R07a are bimodal in size (Fig. 4.4) and both generations show more regular zoning patterns than those in sample R01f. The 'old' garnet displays a normal zoning pattern and the 'new' garnet shows the flat-line profile of a homogenized grain.

The garnet in sample R13 has an irregular profile demonstrating disequilibrium. Discretion is necessary when using pressure and temperature estimates from this sample. Zoning appears in PPL as shades of red.

Clinopyroxene forms large (up to 80 mm) poikiloblastic grains replaced by hornblende to varying degrees. Clinopyroxene grains with relict idioblastic grain boundaries are present in sample R09a. Compositions within individual thin sections are homogenous, but differences are evident from thin section to thin section, with R13 having the most Fe-rich compositions (R01f: Wo_{46}, En_{36}, Fs_{13-16}, and Jd_{1-2}; R07a: Wo_{46}, En_{36-39}, Fs_{8-10}, and Jd_{0-2}; R13: Wo_{45-47}, En_{28-30}, Fs_{17-19}, and Jd_{1-3}).

Quartz is rare, except where it forms veinlets or lenses. Carbonate, epidote, and scapolite appear in amphibolite located near calc-silicate pods or adjacent to anorthosite, monzogranite, or orthogneiss. Orthopyroxene may be present as relict grains.

A broad spectrum of deformation exists in these rocks with samples ranging from nearly mylonitic to massive. Most amphibolite thin sections display a moderate to strong component of deformation, corresponding to the outcrop macrotexture (Fig. 3.4). Shearing is expressed by preferred grain orientation in plagioclase, hornblende, and biotite, and by undulose extinction in quartz. Plagioclase coronas have recrystallized grains attenuated parallel to the stretching lineation.

In every thin section, plagioclase and hornblende replace garnet and clinopyroxene. Moderately fractured and embayed garnets with thin coronas are usually associated with significant quantities of clinopyroxene (Sample R01f). In samples where plagioclase has almost completely replaced garnet, clinopyroxene is rare, having been almost completely replaced by hornblende.

Sample R04, with large, relatively pristine clinopyroxene and rare garnet fragments, is an exception.

A strong correlation exists between the degree of deformation in the samples and the extent to which these reactions have progressed. Samples with remnant garnet, wide plagioclase coronas, and little clinopyroxene exhibit a higher degree of strain than do samples with plentiful clinopyroxene, unreacted garnet, and thin coronas.

4.2.2 Meta-eclogite

An eclogite is a granular rock, composed of garnet (almandine-pyrope) and sodic-pyroxene ± rutile and quartz. Garnet-clinopyroxene rocks at Arnstein and other localities in the Central Gneiss Belt are interpreted as eclogites partially re-equilibrated under granulite to amphibolite facies conditions, and are therefore described as meta-eclogites (Davidson 1991). The Arnstein meta-eclogite has cores of relict kyanite in corundum-spinel-sapphirine symplectite intergrown with bytownite. It is interpreted as derived from a kyanite eclogite. Jadeite concentrations in clinopyroxene in the meta-eclogite are too low for an eclogite, however, they may result from the retrograde breakdown of omphacite to form a plagioclase and calcic clinopyroxene intergrowth (Davidson et al. 1982). Plagioclase-clinopyroxene intergrowths are present in amphibolite and meta-eclogite samples.

In these samples the assemblage is Fe-Ca rich garnet, plagioclase, orthopyroxene, clinopyroxene (as intergrowth with plagioclase), quartz, oxides, corundum/sapphirine/spinel/Ca-plagioclase symplectite ± corundum, kyanite, biotite, rutile, titanite, and hornblende. Kyanite is not always present in thin section but occurs in layers in most hand samples (Fig. 4.6). Garnets are pyrope and grossular-rich, almandine-poor (Alm_{36-44}, Pyr_{30-41}, $Gros_{20-25}$), as is typical of eclogite garnet; andesine (An_{28-44}) and diopside (Wo_{42-44}, En_{42-43}, Fs_{5-7}, Jd_{3-4}) are the other major phases. Biotite grains are very similar in composition with Fe/(Fe+Mg) 0.27-0.28. Hornblende varies from edenitic to pargasitic hornblende with Fe/(Mg+Fe) 0.24-0.31.

Symplectites in these samples contain intergrowths of corundum with Ca-plagioclase, sapphirine with Ca-plagioclase (An_{90-95}), and spinel with Ca-plagioclase. The different types are indistinguishable in thin section, but backscatter images suggest that corundum symplectite overprints spinel symplectite and perhaps sapphirine symplectite (Jamieson, pers. comm.). Figure 4.7 shows a typical symplectite mantled by a plagioclase corona, the whole surrounded by clinopyroxene-plagioclase intergrowth.

Kyanite is present at the cores of some symplectite coronas. Corundum, sapphirine, kyanite, symplectite, and rutile, where present, are locally adjacent to garnets.

Poikiloblastic pyroxene-plagioclase intergrowths are abundant (Fig. 4.8). If they resulted from the breakdown of

omphacitic clinopyroxene (e.g. Davidson 1990), the protolith would have been a true eclogite.

Clinopyroxene forms rims on orthopyroxene and is less poikiloblastic than clinopyroxene. Hornblende has replaced both orthopyroxene and clinopyroxene. Biotite occurs where there are quartz veinlets and lenses, and locally grows on clinopyroxene.

Inclusion-rich garnets are moderately embayed but do not form porphyroblasts as in the Armer Bay amphibolites. Granoblastic plagioclase coronas envelop garnet and symplectite (Fig. 4.8).

Samples R14f and R14g, located near a pegmatite, are largely amphibolitized. R14f is a garnet amphibolite while R14g, nearer the pegmatite, contains very rare garnet.

All the hand samples are fine-grained, slightly foliated, but fairly homogenous except for plagioclase and kyanite layers.

The macroscopic foliation (Fig. 4.9) is not evident at the microscopic scale.

4.2.3 Anorthosite

The dominant phases in the anorthosite are plagioclase, biotite, and opaque minerals, with local hornblende porphyroblasts ± titanite, allanite, zircon, garnet, scapolite, epidote, and relict orthopyroxene.

Two anorthosite samples (R07b and R09b) contain fine-grained plagioclase (An_{30}) and biotite with rare hornblende porphyroblasts ± quartz. Biotite (Fe/(Fe+Mg) 0.55-0.57) and

Fig. 4.6 Meta-eclogite with surface layer containing large kyanite grains. Arnstein (Ketchum 1990).

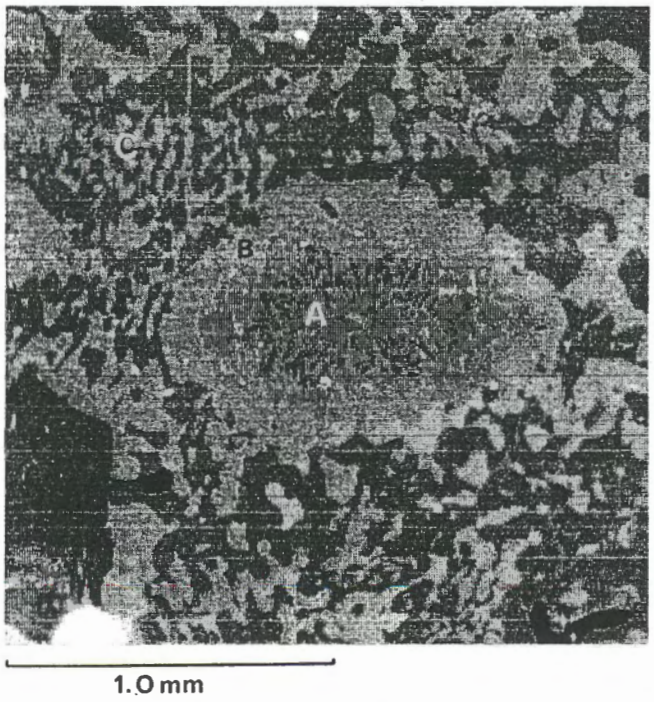

Fig. 4.7 Meta-eclogite. Reversed backscatter electron image of **A** plagioclase corona separating **B** symplectite and **C** clinopyroxene-plagioclase intergrowth. Arnstein.

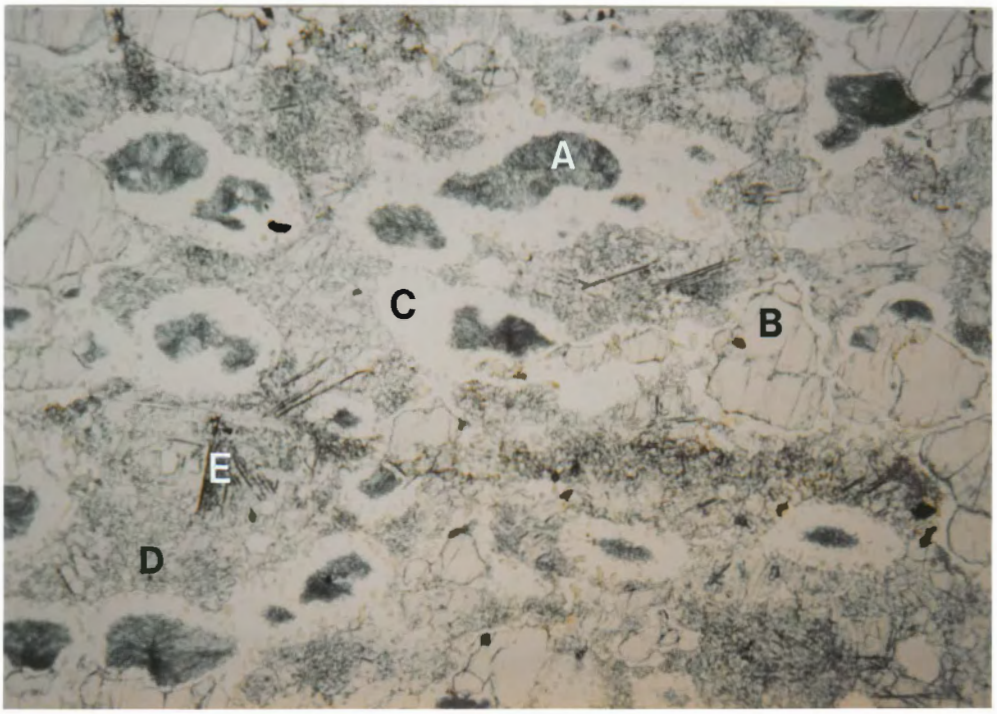

Fig. 4.8 Meta-eclogite showing **A** symplectite and **B** garnet mantled by **C** plagioclase coronas. Matrix is **D** clinopyroxene-plagioclase intergrowth. **E** Relict pyroxene cleavage. Sample R14d, Arnstein. 4x6 mm.

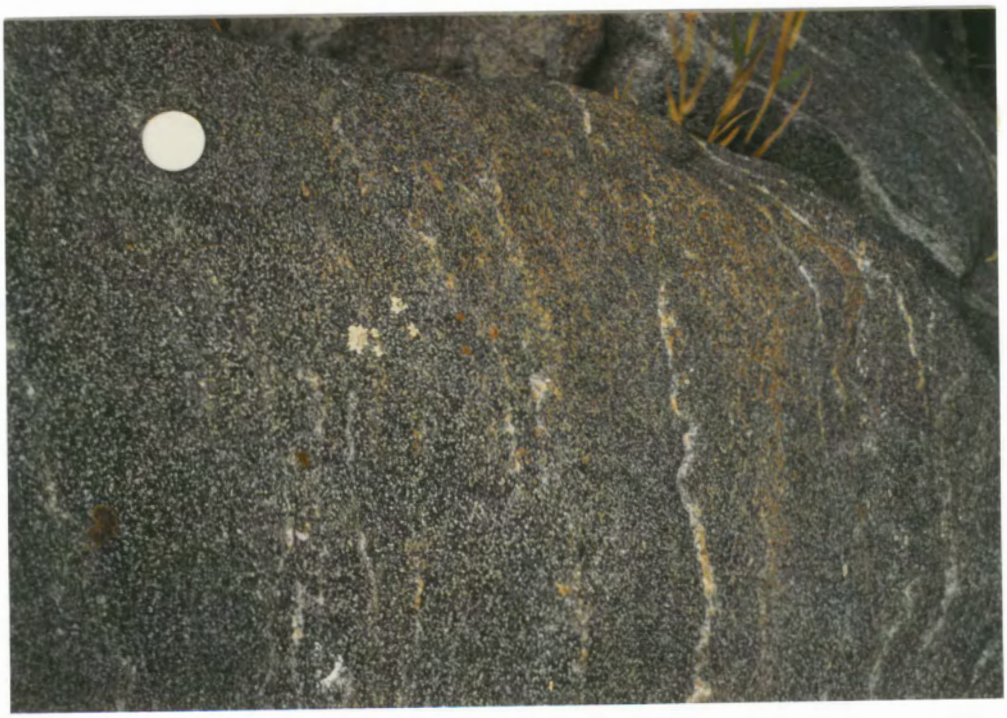

Fig. 4.9 Meta-eclogite displaying slight foliation. Arnstein (Ketchum 1990).

amphibole (ferroan hornblende to pargasitic ferroan hornblende with Fe/(Fe+Mg) 0.62-0.68) are both homogeneous. Garnet is rare. The samples differ in that sample R07b has very minor allanite (in hornblende), opaque grains (ilmenite?), and zircon. Sample R09b has epidote, large biotite grains growing on hornblende, and texturally bimodal scapolite as large, xenoblastic grains and smaller, prismatic grains.

Sample R10 is from an interlayered anorthosite/amphibolite rock. The anorthosite layers consist of plagioclase and biotite with minor scapolite and relict orthopyroxene. The amphibolite layers contain hornblende, plagioclase, and highly disaggregated garnet.

All three samples show a greater degree of strain than the amphibolite samples. Sample R07b has a nearly mylonitic fabric while the other two are strongly foliated. All samples are fine-grained with biotite, epidote, and hornblende grains oriented parallel to the fabric. Some partitioning into mafic and leucocratic layers is evident and the plagioclase grains are recrystallized. The possible presence of relict orthopyroxene in these rocks indicates deformation and metamorphism in granulite facies (Yardley 1989), as does the presence of scapolite (Moecher and Essene 1990).

Information from petrography, combined with microprobe data, determined the direction of geothermobarometry studies. Spatial relationships between phases, observed reaction textures, chemical analyses of individual grain points, mineral chemistry

trends within grains, and quality of microprobe analyses, all combined to suggest the most useful combinations of analyses for particular thermometers and barometers discussed in Chapter 5.

CHAPTER 5 - METAMORPHIC P-T CONDITIONS AND GEOTHERMOBAROMETRY

5.1 Metamorphic P-T Conditions

Phase relations in the Parry Sound amphibolite are consistent with retrograde metamorphism. Various stages of the Cpx + Gnt + H_2O = Plag + Hb reaction are 'frozen in' in these samples. The garnet-plagioclase component of the reaction is a decompression reaction common to granulites and eclogites, and the clinopyroxene-hornblende component is a retrograde hydration reaction (Barker 1990). Some samples (R06, R13) have abundant clinopyroxene and garnet with thin plagioclase coronas and relatively less hornblende, and exhibit little strain. Others (R01h, R02b) have remnants of garnet, wide plagioclase coronas, no clinopyroxene, and abundant hornblende. Sample R01d has no clinopyroxene or garnet and has a protomylonitic fabric. Samples showing two ends of the strain/reaction continuum are present in the same outcrop, indicating locally variable strain, perhaps influenced by fluctuating fluid effects.

Mineral compositions reflect this spectrum of degrees of reaction. Amphibole compositions are heterogenous, implying mineral reaction under changing conditions, and garnet compositions also show disequilibrium effects. Clinopyroxene compositions have the highest jadeite component in the least retrograded sample, again suggesting higher former P-T conditions.

Some samples have lower metamorphic assemblages with biotite overprinting hornblende. Biotite growth is most pronounced in samples from outcrops with quartz veining, constituting further evidence of the control of fluids on these reactions.

Rare remnant grains of orthopyroxene may be present, although a microprobe search was unsuccessful. Any orthopyroxene has most likely been replaced by hornblende.

Figure 5.1 shows the P-T area of the reactions occurring in these rocks, with the arrow indicating the direction of reaction. Relict phases are on the high P-T side of the curve. The garnet to plagioclase component of this reaction is pressure dependent, influencing the slope of the curve. Actual pressure values vary considerably, depending on compositions of the phases involved. The pyroxene to hornblende component of the reaction is more temperature dependent, as illustrated in Figure 5.1 along the granulite- to amphibolite-facies transition curve. This diagram suggests a reaction involving the hydration of an eclogite, either directly to an amphibolite-facies rock or to a granulite facies rock during decreasing pressure and increasing temperature. Subsequent retrogression to amphibolite facies would occur with decreasing temperature or decreasing temperature and pressure. Geochronological data (Table 3.2) imply a relatively long period of time, ca. 55 Ma, over which retrograde metamorphism occurred in this region.

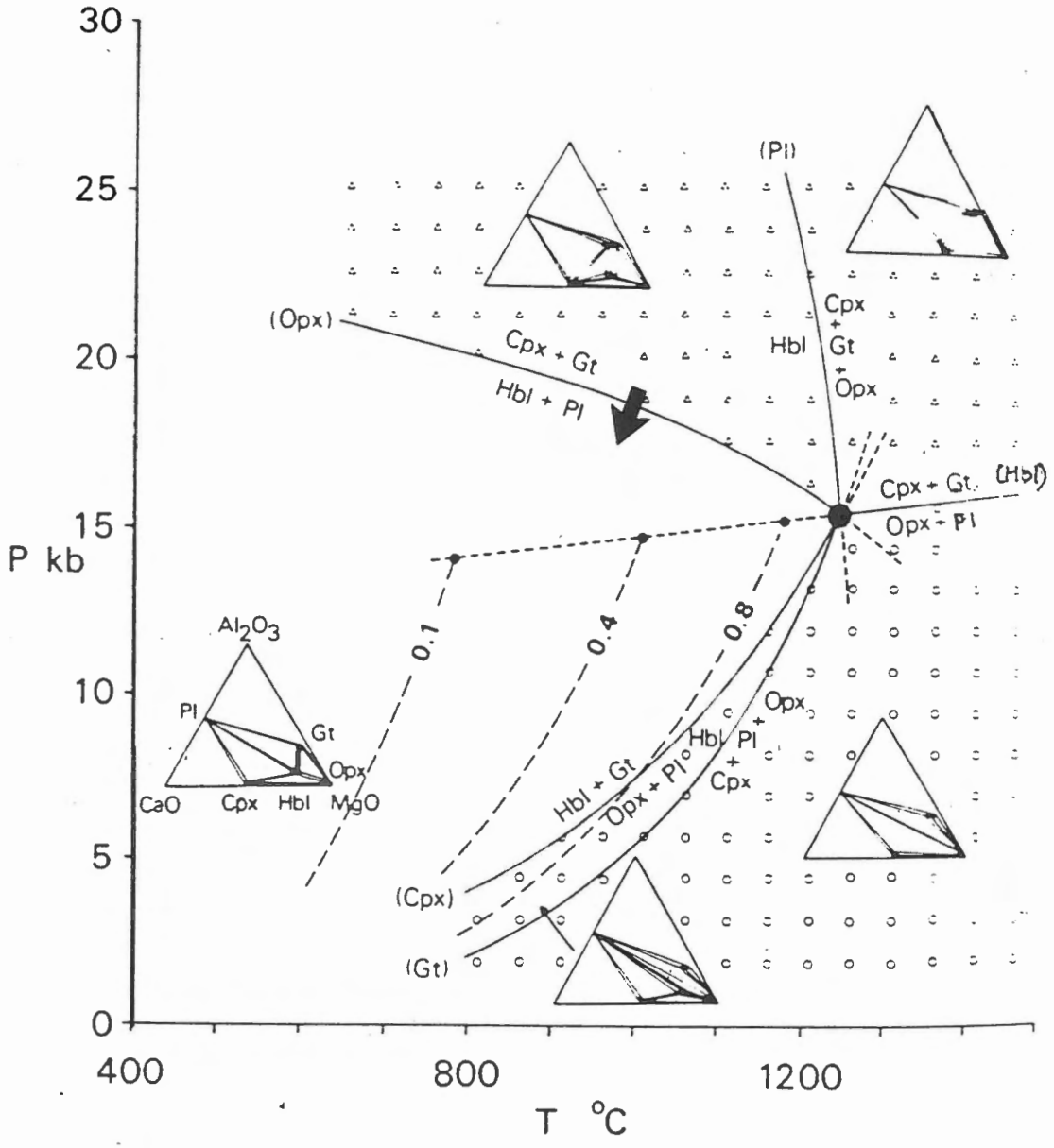

Fig 5.1 Phase relations in part of the system CaO-MgO-Al_2O_3-SiO_2-H_2O with excess SiO_2 and H_2O. Eclogite and granulite stability fields are shown by open triangle and open circle ornament respectively; amphibolite facies stability field is not ornamented. Dashed lines are isopleths of X_H2O for reaction (Gt). Arrow shows direction of reaction observed in amphibolite (after Wells 1979). Note: reaction occurs over wide range of pressures, depending on compositions of phases involved.

5.2 Thermobarometry

The fundamental assumption underlying geothermobarometric calculations is that mineral assemblages were in equilibrium. This poses a problem for P-T determinations on rocks with textural evidence of disequilibrium. During retrogression, intra/inter-crystalline diffusion produces re-equilibration, so that the calculated P-T values do not represent 'peak' metamorphic conditions. The presence of a fluid phase enhances the diffusion effect (Yardley 1989). Later metamorphic events can overprint the phases present.

Added to these difficulties are errors in microprobe analyses, as well as errors inherent in the geothermometer or geobarometer employed. For example, analyses yield only total Fe concentrations, usually given as Fe^{2+}, an assumption that is inaccurate for most Fe-bearing minerals.

It is important, therefore, to select phases that appear to be in equilibrium with each other before applying geothermobarometric techniques, and to take estimates of analytical error into account. Textural evidence and mineral chemistry in these samples suggest that P-T estimates from the garnet amphibolite stage of metamorphism may be possible, but that data bearing on an earlier metamorphic history probably cannot be obtained.

Several phases present in the garnet amphibolite are suitable for geobarometric and geothermometric determinations. Garnet, hornblende, plagioclase, and clinopyroxene analyses from

three samples (R01f, R07a, and R13) were used in geothermometers and geobarometers available via PTLEO and PTt/030 computer programs. In all calibrations Fe was calculated as Fe^{2+} for consistency between formulations, and results therefore represent temperature maxima.

The samples selected are from different locations and exhibit different stages of retrograde reaction. One of the primary factors in analysis choice was garnet zoning; rim-to-core analyses provided potentially significant information regarding changing pressures and temperatures. The proximity of plagioclase, amphibole, and clinopyroxene grains vis-a-vis each other and selected garnets determined the choice of analyses for these minerals. Geothermobarometric calibrations used both matrix and corona plagioclase data as well as rim and core data from plagioclase and clinopyroxene grains. In sample R01f, five core and rim garnet analyses, combined with three plagioclase, one clinopyroxene and two hornblende analyses, gave results listed in Appendix III. Pressure and temperature data from sample R07a are based on analyses from two garnets, core and rim, two plagioclase grains and one clinopyroxene, core and rim, and three hornblendes. Estimates from sample R13 are based on analyses from one garnet and one clinopyroxene, core to rim, and one plagioclase and one hornblende.

Some of the calibrations using plagioclase had to be rejected because of poor analyses; the P-T data for these garnets are based solely on matrix plagioclase.

5.2.1 Geothermometers and Geobarometers

Brief descriptions of the geobarometers and geothermometers employed are below. Details of calibrations and assumptions and limitations are in Appendix III. Unless otherwise stated, errors are ± 50 °C and ± 1 kbar (e.g. Essene, 1989).

1) The garnet-hornblende geothermometer of Graham and Powell (1984) is based on the Fe-Mg exchange reaction between hornblende (pargasite) and garnet. Application of this geothermometer is limited to a maximum of 850 °C, suitable for amphibolite to granulite facies rocks. At higher metamorphic grades the Mg-Fe partitioning between hornblende and garnet phases is non-ideal.

2) The garnet-clinopyroxene geothermometer of Ellis and Green (1979) produces relatively low temperatures from rocks in the low-T eclogite facies. The error is ± 30-50°C or ± 5% of estimated temperature (Jamieson 1990).

3) The garnet-plagioclase-pyroxene-quartz geobarometer of Newton and Perkins (1982) produces results that are relatively insensitive to temperature. Errors of ± 100°C produce pressure errors ranging from a few to several hundred bars. Newton and Perkins find the clinopyroxene barometer (used here) produces an error of ± 1.6 kbar.

The computer program PTLEO generates a simultaneous solution geothermobarometer combining the garnet-clinopyroxene geothermometer of Ellis and Green (1979), and the Newton and Perkins (1982) garnet-plagioclase-clinopyroxene-quartz formulation.

4) The four garnet-hornblende-plagioclase-quartz geobarometers of Kohn and Spear (1989) for garnet amphibolites and granulites rely on reactions involving quartz, plagioclase, garnet, and tschermak exchange in amphibole (hornblende). A combination of accuracy and precision factors suggests that the calculated pressures have an accuracy not better than ± 5 kbar (Kohn and Spear 1989).

5) The garnet-clinopyroxene Fe-Mg exchange thermometer for garnet amphibolites, granulites, and eclogites with low-Na clinopyroxene (Pattison and Newton 1989) has the advantage of being based on reversed experiments. The results are as much as 60-150 °C lower than the Ellis and Green (1979) calibration.

5.2.2 Pressure and Temperature Results

The results of these geothermobarometric calculations are in Table 5.1 and detailed in Appendix IV. The matrix plagioclase formulations produced slightly higher temperature and pressure estimates than corona plagioclase formulations. The combination of garnet rim with matrix plagioclase - probably the best equilibrated combination - produce the most reliable results.

The Newton and Perkins (1982) calibrations yield the lowest pressures for each sample, corresponding to the known error described above for this formulation. The Kohn and Spear (1989) pressure results are usually the highest.

The Graham and Powell (1984) formulation gave results consistent with the Ellis and Green (1979) data. The Pattison and Newton (1989) temperatures are calibrated against the Ellis and Green (1979) temperatures and form the lower temperature limit for these samples, as expected from the known tendency of this geothermometer.

Calibrations yielding the most consistent temperatures and pressures are the Graham and Powell (1984) and Ellis and Green (1979) geothermometers, and the Newton and Perkins (1982) geobarometer. The simultaneous solution P-T estimates are also compatible.

The Kohn and Spear (1989) pressures and Pattison and Newton (1989) temperatures yielded unreasonably low results with respect to other data.

The three samples provided sufficiently different P-T information to be considered separately below.

5.2.2.1 Sample R01f

Five individual garnet porphyroblasts in this sample show different characteristics. Some of the garnets gave higher pressures and temperatures in the cores while others gave higher values in the rims. The P-T results, together with the embayed appearance of most of the garnets, indicate a sample in disequilibrium. However, three of the garnets are homogenous with similar textures, core-rim zoning, and P-T estimates. Their core

TABLE 5.1

Pressure and Temperature Estimates

Sample R01f

Degree of Garnet Embayment

Weak	595 - 610 ± 50 °C	4.5 - 5.5 ± 1.6 kbar
Moderate	620 - 688 ± 50 °C	5.1 - 6.5 ± 1.6 kbar
Strong	610 - 666 + 50 °C	5.7 - 7.4 + 1.6 kbar

Sample R07a

'Old' Garnet	552 - 695 + 50 °C	6.4 - 6.7 + 1.6 kbar
'New' Garnet	690 - 745 + 50 °C	6.7 - 7.3 + 1.6 kbar
Sample R13	726 - 834 + 50 °C	6.3 - 6.4 + 1.6 kbar

Summary of:
1 Graham and Powell (1984) geothermometer.
2 Ellis and Green (1979) geothermometer.
3 Newton and Perkins (1982) geobarometer.
4 simultaneous solution of 2 and 3.

and rim temperatures and pressures fall within the same range of 620-688 °C (± 50 °C) and 5.1-6.5 kbar (± 1.6 kbar error).

A relatively pristine ('unembayed' in Appendix III) garnet gives a somewhat different range of 595-610 °C (± 50 °C) and 4.5-5.5 kbar (± 1.6 kbar), whereas the most corroded garnet gives estimates of 610-666 °C (± 50 °C) and 5.7-7.4 kbar (± 1.6 kbar).

A comparison between the three homogeneous garnets and the other two garnets reveals increasing pressures with increasing embayment. Those garnets that grew during higher pressure conditions are less in equilibrium with more recent, lower pressure conditions.

5.2.2.2 Sample R07a

There are two distinct garnets in this sample: large, highly reacted porphyroblasts, and smaller pristine grains. The 'Old' garnet porphyroblast has yielded temperatures and pressures from 552-695 °C (± 50 °C) and 6.4-6.7 kbar (± 1.6 kbar).

The 'New' garnet produced higher values overall. Temperature and pressure estimates are from 690-745 °C (± 50 °C) and 6.7-7.3 kbar (± 1.6 kbar).

5.2.2.3 Sample R13

One representative garnet gave the highest temperature and pressure results of the three samples, with a range of 726-834 °C (± 50 °C) and 6.3-6.4 kbar (± 1.6 kbar). These results,

especially the pressure results, appear uniform, but considerable variation suggests disequilibrium in this sample.

5.3 Interpretation

Figure 5.2 shows the P-T conditions indicated by geothermobarometry results from the Parry Island amphibolite. These data fall within the P-T path (Fig. 5.3) for meta-pelites from the Parry Island thrust sheet. Garnet-plagioclase-Al_2SiO_5-Quartz barometry (Newton and Hazelton 1981, Koziol and Newton 1988) gives pressures from 7.5-8.5 kbar in kyanite-bearing gneisses, and 4.8-6.0 kbar in kyanite and sillimanite-bearing gneisses from the Parry Island thrust sheet (Jamieson et al 1991). Anovitz and Essene (1990) have published P-T conditions of <730 °C and about 8 kbar for this unit, and have described a thermal high of 800 °C for the Parry Sound area.

Grant (1989) found that temperatures from garnet-clinopyroxene thermobarometry are too low in this region, particularly from coronite metagabbros. This effect may be the result of resetting during cooling and uplift; Fe-Mg cation distribution must have re-equilibrated syn- and post-thrusting.

Small, local variations in pressures and temperatures are attributed by Anovitz and Essene (1986) to small thermal discontinuities. Grant believes that different fluid activities are also responsible. Evidence from this thesis suggests that both mechanisms have influenced the amphibolite.

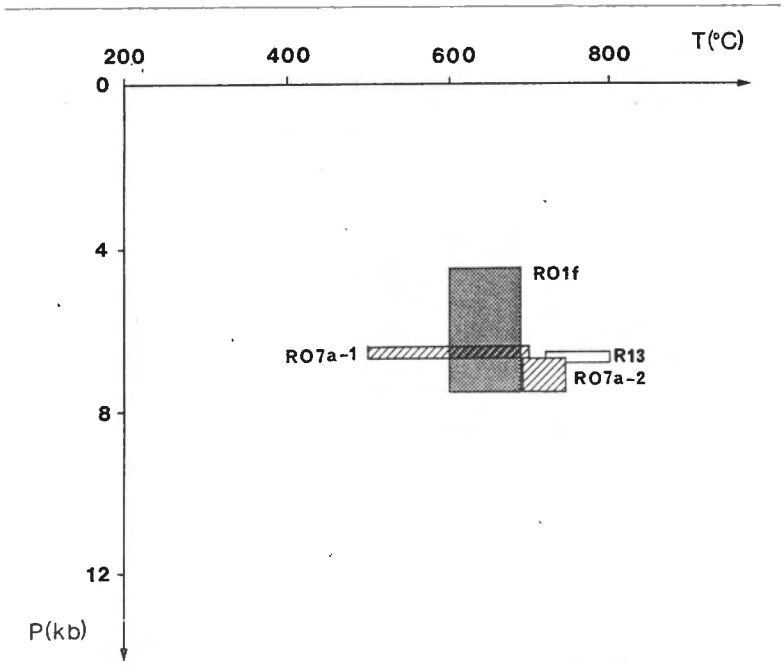

Fig. 5.2 P-T data from 3 samples in the Parry Island amphibolite. **R07a-1** = data based on retrograde garnet, **R07a-2** = data based on second generation garnet. **Note:** data do not include error.

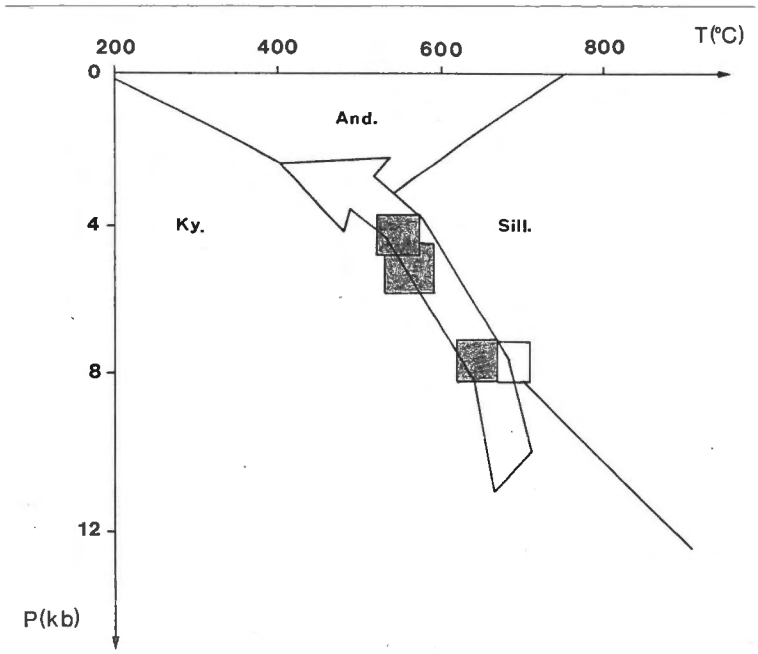

Fig. 5.3 Generalized P-T-t path for the Parry Sound domain. P-T ranges estimated from thermobarometry of unit 3 metapelite assemblages. Shaded box, Jamieson et al. 1991; open box, Anovitz and Essene 1990. Aluminosilicate stability fields after Holdaway (1971). (after Jamieson et al. 1991).

The significance of these results with respect to textural information will be discussed further in Chapter 6.

CHAPTER 6 - DISCUSSION

6.1 Introduction

The objectives of this thesis are to determine pressure and temperature estimates indicative of the metamorphic history of these rocks, and to discover if the Parry Island amphibolite experienced an earlier granulite or eclogite facies history. Geothermobarometric data place the amphibolite along a retrograde P-T path, but petrological, chemical and textural information is important in assessing the former metamorphic history of these rocks.

6.2 Granulite Facies Metamorphism

Texturally and compositionally the amphibolite provides evidence of an earlier, higher P-T history. Some garnets display fluctuation in chemical zoning indicative of disequilibrium. Other garnets, however, are less embayed and provide consistent zoning and P-T data. These garnets have equilibrated at ~650 °C (± 50 °C) and 6 kbar (± 1.6 kbar). Because these rocks are clearly retrograded, the implication is that peak metamorphic conditions for these samples must have been higher. One of the samples, R13, did not experience as much strain as the other samples and is less retrograded. Temperatures and pressures from this sample are about 800 °C (± 50 °C) and 6.4 kbar (± 1.6 kbar). These data may be unreliable because of evident disequilibrium, but a general connection exists between less retrogression and higher P-T conditions. Garnets from sample R01f show higher

pressures from the most embayed garnets, implying relatively earlier garnet growth at higher pressure conditions.

The small, idioblastic garnets in R07a give P-T estimates of about 700 °C (± 50 °C) and 7 kbar (± 1.6 kbar). Their appearance suggests later growth, possibly a result of a late pulse of Grenvillian metamorphism.

Some garnets exhibiting normal zoning during increasing pressure have inclusion-free rims (Fig. 6.1). These rims, evident under cross-nicols, testify to a change in growth pattern. The rims may or may not be a product of the same conditions that produced the idioblastic garnets. Temperatures and pressures from the second generation garnets and from the inclusion-free rims are similar within error, but chemical compositions differ.

A relationship exists between type of garnet and location with respect to other phases. All but one of the garnets (the highly embayed garnet) are normally zoned garnets and are associated with hornblende. The embayed, retrograde garnet is within the clinopyroxene-rich part of the thin section, and has a wide plagioclase corona. Both the disaggregated garnet and the enveloping clinopyroxene are relics of higher grade conditions.

Information from other phases supports data from the garnets. Plagioclase mineral chemistry varies from sample to sample (An_{30-75}). Inclusions in R07a garnets exhibit variable An content, as high as An_{72}. Sample R13 has the highest temperature plagioclase. At higher diffusion rates (higher temperatures)

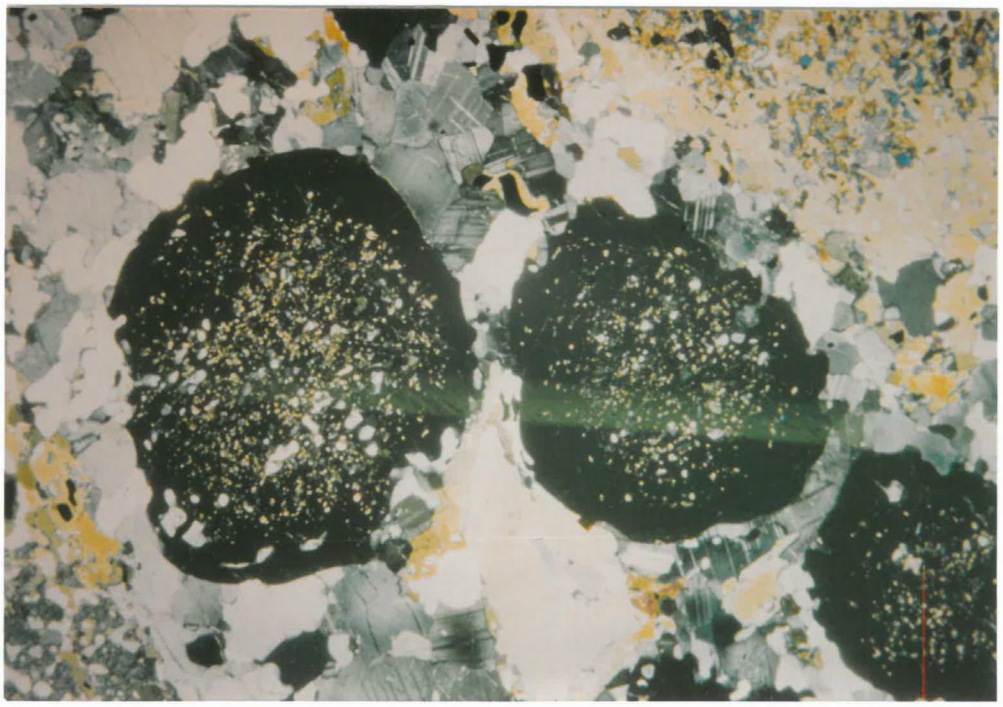

Fig 6.1 Garnet porphyroblasts with inclusion-free rims. Sample R01f, Parry Sound. Cross-nicols. 4 x 6 mm.

plagioclase can be expected to absorb more Ca, and mineral chemistry shows higher Ca content in rims than in cores for all samples.

The presence of orthopyroxene in the amphibolite could not be confirmed, however, this does not preclude a granulite facies history. Yardley (1989) discusses high-pressure granulites lacking orthoypyroxene in plagioclase-bearing clinopyroxene metabasites.

In the meta-eclogites from Arnstein, orthopyroxene occurs at the cores of clinopyroxene grains and appears to have reacted earlier than clinopyroxene to form hornblende. Both pyroxenes are poikiloblastic, but the clinopyroxene is slightly less so than the orthopyroxene. A similar sequence of reaction may have occurred in the amphibolite. However, if orthopyroxene had been present in the Parry Island samples, it would have been completely replaced by hornblende at the P-T conditions experienced by these samples. Orthopyroxene may be present in anorthosite in a sample from the interlayered amphibolite-anorthosite outcrop (R10).

Scapolite is present in the amphibolite and the anorthosite, and is indicative of granulite facies metamorphism. Although uncommon in amphibolites, scapolite is seen in CO_2-rich metabasites (section 4.2.1 Garnet Amphibolite).

Amphibole compositions are similar within and between samples, with the exception of sample R01f. A range of hornblende compositions indicates amphibole growth during changing P-T

conditions and is visible as differing pleochroism (Fig. 4.2). The lighter colour amphibole is characteristic of growth under relatively lower P-T conditions. A minor relative increase in Al_2O_3/SiO_2 and Al^{IV} in sample R13 is again indicative of higher temperatures for this sample.

All of these observations point to former metamorphic conditions in excess of 650 °C, probably within the granulite facies.

6.3 Eclogite Facies Metamorphism

Whether it is possible to project metamorphic conditions back into the eclogite facies is questionable. The metamorphic assemblages and textures in the Armer Bay garnet amphibolites and Arnstein meta-eclogites have certain features in common. Both have plagioclase after garnet and hornblende after pyroxenes. The Gnt + Cpx + H_2O = Plag + Hb reaction has progressed much further in the Armer Bay samples, producing wider plagioclase coronas, embayed and disaggregated garnets, abundant hornblende, and fewer relict pyroxene grains. In the Arnstein samples the orthopyroxene grains show signs of earlier reaction than clinopyroxene, and are rare to non-existent in the Armer Bay samples.

Kyanite, corundum, spinel, and their symplectites do not occur in the Armer Bay amphibolites, but in the Arnstein samples these phases are present with plagioclase coronas. Some of the plagioclase present in the Armer Bay samples may be a product of such reactions.

Both rock types have similar plagioclase-clinopyroxene intergrowths. Jadeite concentrations in clinopyroxene are low; the highest from the amphibolite, at $Jd_{2.6}$, is from sample R13. Arnstein meta-eclogite clinopyroxene has $Jd_{4.2}$. If the Parry Island and Arnstein clinopyroxene-plagioclase intergrowths result from the breakdown of omphacitic clinopyroxene, a former eclogite-facies metamorphism is indicated. However, there is no direct evidence in these rocks that eclogite conditions were ever achieved.

Some indirect evidence that the Parry Island amphibolite could have had an earlier high pressure history comes from the Arnstein meta-eclogite. Two samples near a pegmatite - R14f and particularly R14g - are more like Armer Bay amphibolites than meta-eclogites. They are all composed of plagioclase and hornblende ± garnet, clinopyroxene, titanite and rutile. Figures 6.2 and 6.3 show the similarity between samples from the two areas. The contact between the Arnstein amphibolites and meta-eclogites is gradational. If the meta-eclogite can become an amphibolite through proximity to a pegmatite (i.e., hydration under lower P-T conditions), a similar degree of reaction should be possible in a shear zone.

The Arnstein samples show less evidence of strain than the Armer Bay samples. Armer Bay samples show a correlation between degree of deformation in different areas of the amphibolite, and progression of reactions. Sample R13 apparently comes from a zone in the amphibolite body less affected by retrograde metamorphism.

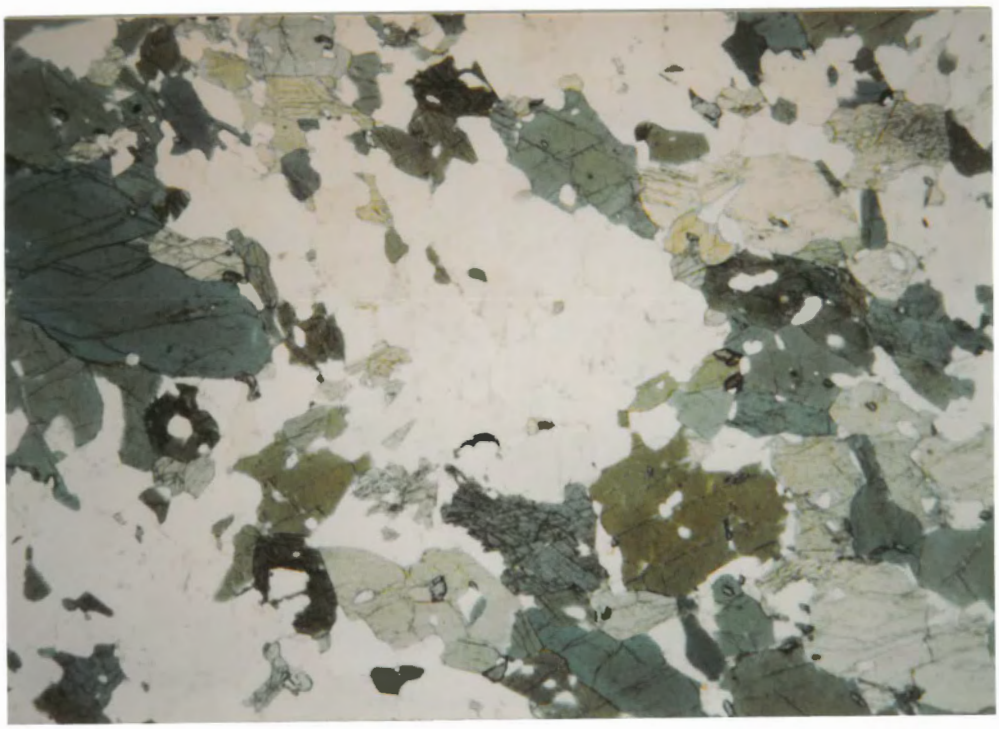

Fig. 6.2 Plagioclase and hornblende in retrograded sample. No garnet or clinopyroxene present. Sample R12a, Rosetta Island, Parry Sound. 4 x 6 mm.

Fig. 6.3 Amphibolitized meta-eclogite. Hornblende and plagioclase. No garnet or clinopyroxene present. Sample R14g, Arnstein. 4 x 6 mm.

Access to fluids might be as important as degree of strain. The Parry Island domain contains abundant pelitic rocks, and the fluids derived from these assemblages would certainly be mobilized in a shear zone and thus available for retrograde reactions. Had the Parry Island rocks not been sheared, an eclogite facies assemblage might have persisted.

The latest P-T conditions of equilibrium probably resulted from a later pulse of Grenvillian thrusting/metamorphism, when the idioblastic, homogeneous garnets grew. Flattened zoning profiles from the garnets also suggest later homogenization at about 650 °C.

CHAPTER 7 - SUMMARY AND CONCLUSIONS

The retrograde (decompression and hydration) reaction Gnt + Cpx + H_2O = Plag + Hb, illustrated by the mineral assemblages and textures of the samples, implies earlier higher P-T conditions. The samples show a clear relationship between the degree of strain and progression of the retrograde reaction. Evidence for a former granulite history includes higher pressure and temperature estimates from a less reacted sample, R13. Garnets in this sample are poorly equilibrated, and P-T data are therefore suspect, but a connection between less retrogression in the samples and higher P-T estimates may be presumed. Mineral chemistry evidence from the same sample includes relatively higher An content in plagioclase, and higher Al_2O_3/SiO_2 and Al^{IV} in hornblende, all indicative of higher former temperatures.

Sample R01f exhibits a correlation between the most extensive embayment in garnets and higher pressures, suggestive of earlier garnet growth under higher pressure conditions.

Plagioclase analyses show high Ca concentrations in rims relative to cores, a feature of higher diffusion rates resulting from higher temperatures. Resorbed garnets and enveloping clinopyroxene-plagioclase intergrowths are also relics of higher grade conditions. The presence of scapolite in amphibolite and anorthosite, and possible presence of orthopyroxene in anorthosite suggests granulite facies metamorphism.

Evidence for a former eclogite facies metamorphism is inconclusive. Both amphibolite and meta-eclogite samples have

clinopyroxene-plagioclase intergrowths being replaced by amphibole. Jadeite content is too low for a true eclogite, but clinopyroxene-plagioclase intergrowths may result from the breakdown of omphacite under decreasing P-T conditions.

Two samples from the meta-eclogite outcrop have been amphibolitized to an assemblage of plagioclase and hornblende with rare garnet, titanite, and rutile. Thin sections reveal a close similarity between these samples and the most retrograded samples from the amphibolite, where clinopyroxene and garnet have been completely replaced by plagioclase and hornblende. The retrograded meta-eclogite is near a pegmatite, implying that the retrogression is the product of hydration under lower P-T conditions. The amphibolite samples may have experienced similar conditions, augmented by high strain. Deformation in the amphibolite is higher than in the meta-eclogite, and is locally variable. A direct correlation exists between the degree of strain seen in the samples and the degree of retrograde reaction observed. The implication is that the amphibolite may have had an eclogite protolith that retrograded through hydration, decompression, and deformation within a shear zone.

The latest metamorphism is expressed by the presence of scapolite, a second generation of pristine garnets, and perhaps by inclusion-free rim growth on earlier garnets. These phases probably result from a later pulse of Grenvillian metamorphism.

Pressure and temperature estimates for the Parry Island amphibolite average 650 °C at 6-7 kbars.

APPENDIX I

Petrological Descriptions

Garnet Amphibolite - Armer Bay, Five Mile Bay, Parry Sound

Mineralogy: Garnet porphyroblasts, plagioclase (matrix and corona), Hornblende, + biotite, clinopyroxene, titanite, quartz, opaque minerals (ilmenite?), scapolite, carbonate, epidote, zircon, muscovite, titanite.

Hand Sample: Massive to foliated. Fine-grained matrix of hornblende, plagioclase + clinopyroxene, biotite, with large (up to 1 cm) garnet porphyroblasts. Plagioclase coronas surround garnets in varying widths. Foliation, where present, results from fine layers of hornblende and plagioclase moderately strained to protomylonitic. Garnets show no sign of strain, plagioclase coronas show progressive strain with increase in corona width. Orthopyroxene, where present, is associated with leucocratic layers. Quartz veins in some samples cut fabric at angles varying from high to sub-parallel to foliation.

Thin Section: Garnet porphyroblasts vary from slightly embayed to highly disaggregated. In some thin sections garnet has virtually gone completely to pladioclase. Numerous inclusions are present. Some sections display inclusion free rims on some grains. Plagioclase is present in the matrix and as coronas enveloping garnets. Width of coronas is dependent of the degree of reaction of Gnt + Cpx = Plag + Hb. Hornblende is replacing clinopyroxene and forms both medium-sixed, (sub) euhedral grains, and poikiloblastic grains. Clinopyroxene, where present is very poikiloblastic and is being extensively replaced by hornblende. There is possible remnant orthopyroxene in two thin sections. Biotite grows on hornblende and rarely on plagioclase and garnet. It is associated with samples with quartz veinlets. Grains are oriented parallel to the thin section fabric. Thin section shows varying degrees of strain in grain preferred orientation of mafic phases, attenuated plagioclase coronas, and recrystallization of plagioclase coronas.

Sample	R01d	High strain, no garnet or Cpx, and abundant plag.
	R01f	No strain, abundant Cpx, thin plag coronas. Bimodal garnet in hand sample, 2-3 mm and 1 cm. Sample up to 45% garnet.
	R04	Carbonate and scapolite present.
	R07a	Bimodal garnet in thin section. Large, embayed porphyroblasts and small, idioblastic grains. High strain in plag rims.

R08b Possible relict Opx in garnet.

R09a Cpx has relict idioblastic grain boundaries. Carbonate present.

R11 Chlorite and alteration present.

R12a No Cpx or garnet, just Hb and plag.

R13 Visible zoning in garnet. No strain, abundant Cpx.

Anorthosite - Armer Bay, Five Mile Bay

Mineralogy: Plagioclase, biotite, hornblende + scapolite, quartz, titanite, epidote, zircon, allanite.

Hand Sample: Well foliated to protomylonitic, fine-grained, composed of plagioclase and boitite and rare hornblende. Scapolite, garnet, and opaque minerals are present locally.

Thin Section: Fabric is defined by the plagioclase and biotite layering and by the orientation of the biotite grains. Biotite also grows on hornblende and epidote where they are present, and rarely on plagioclase.

Sample R09b Bimodal scapolite and epidote present.

R10 Interlayered garnet amphibolite and anorthosite.

Meta-Eclogite - Arnstein

Mineralogy: Garnet, plagioclase (in symplectite and as coronas around garnets and symplectite), corundum/sapphirine/spinel/Ca-plagioclase symplectite, orthopyroxene, clinopyroxene, + kyanite, rutile, corundum, hornblende, quartz, titanite, and biotite.

Hand Sample: Fine-grained, equigranular, homogenous, with leucocratic layers containing kyanite. Slightly foliated.

Thin Section: Corundum symplectites seem to be replacing the spinel and perhaps the sapphirine symplectite. Thin, granoblastic plagioclase coronas envelop garnets and symplectite. Poikiloblastic orthopyroxene and clinopyroxene present with orthopyroxine at core of clinopyroxine. Clinopyroxene may be

replacing orthopyroxene, and hornblende is replacing both. Biotite is associated with quartz lenses and veinlets, and locally grows on clinopyroxene.

Samples R14g,f Located near a pegmatite, they are a garnet, clinopyroxene amphibolite, and an amphibolite respectively. No kyanite, corundum, or symplectite is present.

APPENDIX IIa

Microprobe Analyses for Geothermobarometry - Weight % Oxides

Sample R01f

Garnet

	Probe Analysis Number				
	79(core)	81(rim)	134(rim)	139(core)	160(core)
Oxides					
SiO2	37.56	38.47	39.01	38.50	38.40
TiO2	0.00	0.09	0.00	0.00	0.00
Al2O3	21.28	21.36	20.59	20.55	21.01
Cr2O3	0.11	0.00	0.08	0.00	0.00
FeO	26.07	28.56	27.63	28.32	26.64
MnO	3.10	0.42	0.51	0.64	0.63
MgO	3.13	4.86	3.96	3.84	3.92
CaO	9.03	7.40	8.87	7.59	9.06
Na2O	0.28	0.22	0.00	0.20	0.26
K2O	0.00	0.00	0.00	0.00	0.00
Total	100.56	101.38	100.65	99.64	99.92

	162(rim)	166(rim)	168(core)	173(rim)	174(c-r)
Oxides					
SiO2	37.78	37.76	37.74	37.90	37.85
TiO2	0.00	0.00	0.10	0.07	0.00
Al2O3	20.37	20.84	20.70	20.85	20.74
Cr2O3	0.07	0.00	0.00	0.00	0.00
FeO	28.47	29.33	27.17	27.98	26.93
MnO	0.59	0.65	2.07	0.77	1.66
MgO	3.76	3.13	2.73	3.64	3.30
CaO	7.63	7.81	9.33	8.42	8.89
Na2O	0.18	0.29	0.21	0.22	0.24
K2O	0.00	0.00	0.00	0.00	0.00
Total	98.85	99.81	100.05	99.85	99.69

	175(core)
Oxides	
SiO2	37.78
TiO2	0.00
Al2O3	20.91
Cr2O3	0.00
FeO	27.14
MnO	2.68
MgO	3.13
CaO	8.57
Na2O	0.22
K2O	0.00
Total	100.43

APPENDIX IIa

Microprobe Analyses for Geothermobarometry - Weight % Oxides

Sample R01f (cont.)

Plagioclase	Probe Analysis Number			
	140(corona)	152(matrix)	171(corona)	179(corona)
Oxides				
SiO2	60.78	60.67	59.18	59.07
Al2O3	25.22	24.24	25.03	25.57
FeO	0.00	0.14	0.08	0.27
CaO	7.15	6.30	6.98	7.48
Na2O	6.99	8.23	7.43	7.40
K2O	0.00	0.11	0.07	0.06
Total	100.14	99.69	98.77	99.85

Hornblende			**Clinopyroxene**
	157	172	150
Oxides			
SiO2	45.55	42.57	53.78
TiO2	0.69	1.12	0.13
Al2O3	9.22	12.35	0.76
Cr2O3	0.12	0.10	0.11
FeO	16.33	16.43	10.26
MnO	0.00	0.00	0.00
MgO	11.02	9.82	12.56
CaO	11.51	11.38	22.79
Na2O	1.82	2.25	0.60
K2O	0.40	0.60	0.00
Total	96.66	96.62	100.99
Name	Edenite	Ferroan-Parg.Hb.	

APPENDIX IIa

Microprobe Analyses fro Geothermobarometry - Weight % Oxides

Sample R07a

Garnet

	Probe Analysis Number			
	4(rim)	7(core)	23(core)	25(rim)
Oxides				
SiO2	37.96	37.98	38.23	38.18
TiO2	0.12	0.00	0.00	0.00
Al2O3	21.03	20.89	21.07	20.83
Cr2O3	0.00	0.00	0.00	0.00
FeO	23.78	22.63	24.45	24.40
MnO	1.77	3.13	1.46	1.56
MgO	3.74	2.65	4.24	3.91
CaO	11.32	12.29	10.62	11.38
Na2O	0.10	0.00	0.20	0.23
K2O	0.00	0.04	0.00	0.00
Total	99.82	99.61	100.27	100.49

Plagioclase

	12(corona -rim)	13(corona -core)	28(corona -rim)	29(corona -core)
Oxides				
SiO2	56.70	57.52	57.16	58.74
Al2O3	27.15	26.57	27.23	25.98
FeO	0.09	0.08	0.32	0.00
CaO	9.39	9.04	9.69	8.07
Na2O	5.52	5.61	5.76	6.41
K2O	0.06	0.08	0.07	0.07
Total	98.91	98.90	100.23	99.27

Hornblende				**Clinopyroxene**	
	18	26	27	41(rim)	42(core)
Oxides					
SiO2	42.47	41.94	42.28	52.25	51.26
TiO2	1.24	1.39	1.31	0.16	0.23
Al2O3	12.93	12.72	12.69	1.97	2.95
Cr2O3	0.10	0.00	0.12	0.00	0.08
FeO	16.33	16.20	15.97	9.55	9.75
MnO	0.13	0.08	0.13	0.00	0.17
MgO	10.50	10.11	10.49	12.91	11.97
CaO	12.11	12.07	11.85	23.92	23.52
Na2O	2.02	1.86	1.91	0.65	0.82
K2O	0.50	0.51	0.49	0.00	0.00
Total	98.33	96.88	97.24	101.41	100.75
Name	Ferroan-Parg.Hb.	Ferroan-Parg.Hb.	Ferroan-Parg.Hb.		

APPENDIX IIa

Microprobe Analyses for Geothermobarometry - Weight % Oxides

Sample R13

Garnet	Probe Analysis Number	
	107(rim)	109(core)
Oxides		
SiO2	38.00	37.69
TiO2	0.00	0.11
Al2O3	20.53	20.19
Cr2O3	0.15	0.00
FeO	22.82	22.53
MnO	0.86	2.14
MgO	1.60	1.58
CaO	16.13	15.39
Na2O	0.16	0.09
K2O	0.00	0.00
Total	100.25	99.72

	Plagioclase	**Hornblende**	**Clinopyroxene**
	196(corona)	121	125(core)
Oxides			
SiO2	46.52	39.69	50.54
TiO2	0.00	0.50	0.13
Al2O3	27.30	14.49	2.70
Cr2O3	0.00	0.00	0.00
FeO	0.27	20.75	13.57
MnO	0.00	0.17	0.14
MgO	0.00	6.35	9.54
CaO	18.46	11.81	22.57
Na2O	3.49	2.16	0.70
K2O	0.00	0.24	0.00
Total	96.04	96.16	99.89
Name		Ferroan-Parg.Hb.	

APPENDIX IIb
Microprobe Analyses for Geothermobarometry - Cations

Sample R07a: Garnet (24 oxygen)

Cations	Garnet #4 rim	Garnet #7 core	Garnet #23 core	Garnet #25 rim
Si	5.98	6.01	5.99	5.98
Al	3.90	3.89	3.89	3.85
Ti	0.01	0.00	0.00	0.00
Fe3+	0.00	0.00	0.00	0.00
Mg	0.88	0.63	0.99	0.91
Fe2+	3.13	3.00	3.20	3.20
Mn	0.24	0.42	0.19	0.21
Ca	1.91	2.08	1.78	1.91
Na	0.03	0.00	0.06	0.07
K	0.00	0.01	0.00	0.00
Zn	0.00	0.00	0.00	0.00
Ni	0.00	0.00	0.00	0.00
Cr	0.00	0.00	0.00	0.00
Total wt. % oxide	99.82	99.61	100.27	100.49

Sample R07a: Plagioclase (8 oxygen)

Cations	Plag #12 corona-rim	Plag #13 corona-core	Plag #28 corona-rim	Plag #29 corona-core
Si	2.56	2.60	2.62	2.56
Al	1.45	1.41	1.38	1.44
Ti	0.00	0.00	0.00	0.00
Fe3+	0.00	0.00	0.00	0.00
Mg	0.00	0.00	0.00	0.00
Fe2+	0.00	0.00	0.01	0.01
Mn	0.00	0.00	0.00	0.00
Ca	0.46	0.44	0.40	0.47
Na	0.48	0.49	0.53	0.50
K	0.00	0.01	0.00	0.00
Zn	0.00	0.00	0.00	0.00
Ni	0.00	0.00	0.00	0.00
Cr	0.00	0.00	0.00	0.00
Total wt. % oxide	98.91	98.9	100.23	99.27

Sample R07a: Clinopyroxene (6 oxygen)

Cations	Cpx #17	Cpx #41 rim	Cpx #42 core
Si	1.92	1.92	1.90
Al	0.10	0.09	0.13
Ti	0.01	0.00	0.01
Fe3+	0.00	0.00	0.00
Mg	0.73	0.71	0.66
Fe2+	0.26	0.29	0.30
Mn	0.01	0.00	0.01
Ca	0.94	0.94	0.93
Na	0.05	0.05	0.06
K	0.00	0.00	0.00
Zn	0.00	0.00	0.00
Ni	0.00	0.00	0.00
Cr	0.00	0.00	0.00
Total wt. % oxide	101.73	101.41	100.75

Sample R07a: Amphibole (24 oxygen)

Cations	Amph #18 Fe Parg. Hbl	Amph #26 Fe Parg. Hbl	Amph #27 Fe Parg. Hbl
Si	6.32	6.34	6.35
Al	2.27	2.27	2.25
Ti	0.14	0.16	0.15
Fe3+	0.00	0.00	0.00
Mg	2.33	2.28	2.35
Fe2+	2.03	2.05	2.01
Mn	0.02	0.01	0.02
Ca	1.93	1.95	1.91
Na	0.58	0.55	0.56
K	0.10	0.10	0.09
Zn	0.00	0.00	0.00
Ni	0.00	0.00	0.00
Cr	0.01	0.00	0.01
Total wt. % oxide	98.33	96.88	97.24

Sample R01f: Garnet (24 oxygen)

Cations	Garnet #160 core	Garnet #162 rim	Garnet #166 rim	Garnet #168 core
Si	6.04	6.05	6.01	6.00
Al	3.89	3.84	3.91	3.88
Ti	0.00	0.00	0.00	0.01
Fe3+	0.00	0.00	0.00	0.00
Mg	0.92	0.90	0.74	0.65
Fe2+	3.51	3.81	3.91	3.61
Mn	0.08	0.08	0.09	0.28
Ca	1.53	1.31	1.33	1.59
Na	0.08	0.06	0.09	0.07
K	0.00	0.00	0.00	0.00
Zn	0.00	0.00	0.00	0.00
Ni	0.00	0.00	0.00	0.00
Cr	0.00	0.01	0.00	0.00
Total wt. % oxide	99.92	98.85	99.81	100.05

Sample R01f: Plagioclase (8 oxygen)

Cations	Plag #152 matrix	Plag #171 corona
Si	2.71	2.67
Al	1.28	1.33
Ti	0.00	0.00
Fe3+	0.00	0.00
Mg	0.00	0.00
Fe2+	0.01	0.00
Mn	0.00	0.00
Ca	0.30	0.34
Na	0.71	0.65
K	0.01	0.00
Zn	0.00	0.00
Ni	0.00	0.00
Cr	0.00	0.00
Total wt. % oxide	99.69	98.77

Sample R01f Clinopyroxene (6 oxygen)

Cations	Cpx #150
Si	2.00
Al	0.03
Ti	0.00
Fe3+	0.00
Mg	0.70
Fe2+	0.32
Mn	0.00
Ca	0.91
Na	0.04
K	0.00
Zn	0.00
Ni	0.00
Cr	0.00
Total wt. % oxide	100.99

Sample R01f: Amphibole (24 oxygen)

Cations	Amph #156 Actin. Hbl	Amph #157 Edenite	Amph #172 Fe Parg. Hbl
Si	7.37	6.85	6.45
Al	0.88	1.63	2.21
Ti	0.04	0.08	0.13
Fe3+	0.00	0.00	0.00
Mg	3.03	2.47	2.22
Fe2+	1.83	2.05	2.08
Mn	0.01	0.00	0.00
Ca	1.82	1.85	1.85
Na	0.30	0.53	0.66
K	0.02	0.08	0.12
Zn	0.00	0.00	0.00
Ni	0.00	0.00	0.00
Cr	0.01	0.01	0.01
Total wt. % oxide	97.58	96.66	96.62

Sample R13: Garnet (24 oxygen)

Cations	Garnet #107 rim	Garnet #109 core
Si	6.00	6.00
Al	3.82	3.78
Ti	0.00	0.01
Fe3+	0.00	0.00
Mg	0.38	0.38
Fe2+	3.01	3.00
Mn	0.12	0.29
Ca	2.73	2.62
Na	0.05	0.03
K	0.00	0.00
Zn	0.00	0.00
Ni	0.00	0.00
Cr	0.02	0.00
Total wt. % oxide	100.25	99.72

Sample R13: Amphibole (24 oxygen)

Cations	Amph #121 Fe Parg. Hbl
Si	6.18
Al	2.66
Ti	0.06
Fe3+	0.00
Mg	1.47
Fe2+	2.70
Mn	0.02
Ca	1.97
Na	0.65
K	0.05
Zn	0.00
Ni	0.00
Cr	0.00
Total wt. % oxide	96.16

Sample R13: Plagioclase (8 oxygen)

cations	Plag #196 corona
Si	2.26
Al	1.56
Ti	0.00
Fe3+	0.00
Mg	0.00
Fe2+	0.01
Mn	0.00
Ca	0.96
Na	0.33
K	0.00
Zn	0.00
Ni	0.00
Cr	0.00
Total wt. % oxide	96.04

Sample R13: Clinopyroxene (6 oxygen)

cations	Cpx #125 core	Cpx #128 rim
Si	1.93	1.96
Al	0.12	0.07
Ti	0.00	0.01
Fe3+	0.00	0.00
Mg	0.54	0.58
Fe2+	0.43	0.40
Mn	0.01	0.01
Ca	0.92	0.95
Na	0.05	0.04
K	0.00	0.00
Zn	0.00	0.00
Ni	0.00	0.00
Cr	0.00	0.00
Total wt. % oxide	99.89	100.52

APPENDIX III

Geothermobarometry Calibration Methods

Garnet-Plagioclase-Pyroxene-Quartz Geobarometer - Newton and Perkins, 1982 (with clinopyroxene)

Chemical Reaction - with Clinopyroxene

$CaAl_2Si_2O_8 + CaMgSi_2O_6 = 2/3Ca_3Al_2Si_3O_{12} + 1/3Mg_3Al_2Si_3O_{12} + SiO_2$
(plag) (diopside) (grossular) (pyrope) (quartz)

P (± 1600 bars) = 675 + 17.179T(K) + 3.5962TlnK, where

$K = (a_{Ca})^2(a_{Mg})/(a_{An})(a_{Di})$
T = "best guess", or can be solved simultaneously with a geothermometer (eg. garnet-clinopyroxene). Relatively insensitive to errors in T - an error of ± 100°C leads to pressure errors of only a few to several hundred bars.

Garnet activities:
for grossular, $RT\ln_{Ca} = (3300 - 1.5T)(X_{Mg} + X_{Mg}X_{Fa})$
for pyrope, $RT\ln_{Mg} = (3300 - 1.5T)(X_{Ca} + X_{Ca}X_{Fa})$
where = activity coefficient, X = mole fraction of each component.

Plagioclase activity:
Activity coefficient of anorthite from Newton et al., 1980.
$RT\ln_{An} = X_{Ab}(W_{An} + 2X_{An}(W_{Ab} - W_{An}))$
where W_{An} = 2025 cal, W_{Ab} = 6746 cal.
activity of anorthite: $a_{An} = {}_{An} \times X_{An}(1+X_{An})^2/4$ (Al-avoidance method).

Pyroxene activities:
Ideal two-site mixing model of Wood and Banno 1973.
$a_{Di} = X_{Ca} \times X_{Mg}$ in clinopyroxene
where M2 contains CA, Na, Mn, and Fe^{2+},
M1 contains Mg, Fe^{3+}, Ti, Al, and remaining Fe^{2+}.

Basis of calibration: thermodynamic calibration based almost entirely on measured thermodynamic quantities using (then) recent data. Cpx reaction first calibrated by Perkins (1979).

Assumptions and limitations: Assumes Δg and ΔV to be constants. ΔV is the 298K, 1 bar volume change. ΔS can only be considered constant over the T range of 850-1150K.

Mn-rich garnets rule out the use of this geobarometer because of uncertainty in the mixing properties of spessartine with other garnet components. Garnets with Mn ≥ Mg/3 are excluded.

Due to partial Al-Si disordering in the tetrahedral site, a configurational entropy of 1 cal/K is added to the entropy of anorthite. The uncertainty in this term adds considerably to the pressure uncertainty or the barometer.

The Margules parameters W_{CaFe} and W_{FeMg} are assumed to equal zero in calculating grossular and pyrope activity coefficients,which leads to the symplified expressions given above.

Calculation of anorthite activity assumes plagioclase crystallization in the high structural state. If invalid, the calculated activity may be incorrect.

The barometer assumes ferrous iron to be the main substituant in enstatite and diopside; however, this will lead to erroneous results when Fe_{2+} is significant.

Comments: Newton and Perkins consistently find this Cpx barometer to yield pressures approximately 2 Kbars lower than their Opx barometer, which agrees more closely with other barometers.

(from survey of barometer by J. Ketchum, 1988)

Garnet-Clinopyroxene Geothermometer - Ellis and Green, 1979.

Chemical reaction:
$1/3Mg_3Al_2Si_3O_{12} + CaFeSi_2O_6 = 1/3\ Fe_3Al_2Si_3O_{12} + CaMgSi_2O_6$
(pyrope) (hedenbergite) (almandine) (diopside)

$$T(°K) = 3104(X_{Ca})^{gnt} + 3030 + 10.86P(kb)/\ln K_D + 1.9034$$

$$X(_{Ca})^{gnt} = Ca/(Ca+Mg+Fe+Mn)$$

P (kb) = best guess at P for required T; can be solved iteratively or simultaneously with a geobarometer (e.g. Gnt-Cpx-Plag-Qtz).

$$K_D = (X_{Fe})^{gnt} \times (X_{Mg})^{cpx}/(X_{Mg})^{gnt} \times (X_{Fe})^{cpx}$$

$X(_{Fe})^{gnt}$, $X(_{Mg})^{gnt}$, $X(_{Fe})^{cpx}$, $X(_{Mg})^{cpx}$: Fe/(Mg+Fe): Mg/(Mg+Fe).

Error not explicitly stated but on the order of ± 30-50°C (or ± 5% of estimated temperature), see Powell, 1985.

Basis of calibration: Experimental calibration (seeded glass) in P range 15-30 kb and T range 750-1300°C. Combined with earlier experimental data (Raheim and Green, 1974, and others) and compared with $(X_{Ca})^{gnt}$ over T range 8000-1500°C.

Assumptions and limitations: Assumes ideality for Fe-Mg substitution; this has recently been shown to be incorrect (Pattison, 1987, 1988) and is likely to yield erroneous T

estimates at low and at high T.

Model corrects for non-ideality of Ca solution in garnet; this correction is itself model-dependent and subject to new information (e.g. Koziol, 1988). Koons (1984)suggests that this thermometer will yield temperatures that are too high when used with jadeite-rich pyroxene (X_{jd} > 70%).

Generally, Fe = Fe^{2+} (total). This can cause serious problems where Fe^{3+} is significant (calculated temperature will be too high); if stoichiometry suggests Fe^{3+} > ~20% of total Fe, suggest correcting for it using Fe^{3+} calculation techinques of Koons (1984) and Mottana (1986) and using lower Fe^{2+} in the equation.

Comments: This thermometer probably yields temperatures that are too low for low temperature eclogites, owing to solid solution, extrapolation, and Fe^{3+} promlems. Pattison (1987, 1988) discusses major problems in Fe-Mg non-ideality, site distribution, etc.

(from survey of thermometer by R. Jamieson, 1988)

Garnet-Hornblende Geothermometer - Graham and Powell, 1984

Chemical reaction:

$1/4NaCa_2Fe_4Al_3Si_6O_{22}(OH)_2$ + $1/3Mg_3Al_2Si_3O_{12}$ =
(ferro-pargasite) (pyrope)

$1/4NaCa_2Mg_4Al_3Si_6O_{22}(OH)_2$ + $Fe_3Al_2Si_3O_{12}$
(pargasite) (almandine)

$T(°K) = 2880 \quad 3280X_{Ca}/\ln K_D + 2.426$

Activity and K_D:
Equilibrium constant $K = (a_{alm}/a_{py})^{1/3} \times (a_{pa}/a_{fe\text{-}pa})^{1/4}$
but for ideal solid solution between hornblende and garnet,
$K = (X_{Fe}/X_{Mg})/(X_{Fe}/X_{Mg}) = K_D$, where K_D is a function solely of temperature and pressure, and where
$X_{Fe} = Fe/(Fe+Mg+Mn+Ca)$
$X_{Mg} = Mg/(Fe+Mg+Mn+Ca)$
$X_{Fe} = Fe/(Fe+Mg)$
$X_{Mg} = Mg/(Fe+Mg)$

Basis of calibration: Limited experimental calibration of garnet/hornblende thermometer over pressure ranges of 15-25 Kb (Essene et al. 1970, Green et al. 1972). These experiments were not conducted on coexisting garnets and hornblendes with two exceptions. Empirical calibration (comparison with garnet-clinopyroxene barometer) over pressures and temperatures of 5-10 Kb and 600-1000°C (see Graham and Powell 1984, table 1,2).

Assumptions and limitations: Assuming ideality of the solid solution between hornblende-garnet is not valid and therefore must be corrected. Non-ideality in Ca-amphibole is presently impossible to isolate. Therefore all non-ideality associated with Ca is assigned to the Ca component of the garnet phase. This manifests itself as X_{Ca} in the final temperature formulation given above. Fe total = Fe^{2+} in the hornblende. This is justified to some extent by a detailed survey of hornblende amphibolites ± a garnet phase where the assemblage with garnet shows significantly lower Fe^{3+} values than does the garnet-absent assemblage.

The thermometer is limited to maximum temperatures of 850°C because of closure problems. Due to Fe^{2+}/Fe^{3+} relations in hornblende, the application is used for rocks formed at low O_2 activities.

Although co-existing garnets should not exceed $X_{Mn} > 0.1$, the thermometer is applicable over a wide range of common hornblende.

Comments: May be used on amphibolite to granulite facies rocks. Eclogite compositions usually fall outside of applicability since Fe/Mg partitioning between hornblende-garnet phases is fairly non-ideal at such extremes.

(from survey of thermometer by M. Hendriks, 1988)

APPENDIX IV

Geothermometry and Geobarometry Results

Sample R01f
'Unembayed' Garnet - Core
Gnt 168(core), Plag 171(corona), Cpx 150, Hb 172

Graham and Powell		613 °C				
Pattison and Newton	at	6.5 Kb	= 436 °C		8 Kb	= 445 °C
		7	= 439		8.5	= 447
		7.5	= 442		9	= 450
Newton and Perkins	at	700 °C	= 5.5 Kb			
Simultaneous Solution		610 °C,	5.1 Kb			
Ellis and Green	at	5 Kb	= 610 °C		8 Kb	= 618 °C
		6	= 613		9	= 620
		7	= 615		10	= 623

Gnt 168(core), Plag 152 (matrix), Cpx 150, Hb 172

Kohn and Spear	at	400 °C	= 6.8 Kb		600 °C	= 9.8 Kb
(model 2 Mg)		450	= 7.5		650	= 10.5
		500	= 8.3		700	= 11.3
		550	= 9.0			
Newton and Perkins	at	700 °C	= 6.1 Kb			
Simultaneous Solution		612 °C,	5.6 Kb			

'Unembayed' Garnet - Rim
Gnt 166 (rim), Plag 171(corona), Cpx 150, Hb 172

Graham and Powell		595 °C				
Kohn and Spear	at	400 °C	= 6.1 Kb		600 °C	= 8.8 Kb
(model 2 Mg)		450	= 6.8		650	= 9.5
		500	= 7.5		700	= 10.1
		550	= 8.1			
Pattison and Newton	at	4 Kb	= 404 °C		7 Kb	= 420 °C
		4.5	= 406		7.5	= 422
		5	= 409		8	= 426
		5.5	= 412		8.5	= 428
		6	= 415		9	= 431
		6.5	= 417			
Newton and Perkins	at	700 °C	= 4.9 Kb			
Simultaneous Solution		593 °C,	4.5 Kb			
Ellis and Green	at	4 Kb	= 592 °C		7 Kb	= 599 °C
		5	= 594		8	= 602
		6	= 597		9	= 604

Gnt 166(rim), Plag 152(matrix), Cpx 150, Hb 172

Newton and Perkins	at	700 °C	= 5.5 kb
Simultaneous Solution		594 °C,	4.9 Kb

APPENDIX IV

Geothermometry and Geobarometry Results

Sample R01f (continued)
'Embayed' Garnet - Core
Gnt 160(core), Plag 171(corona), Cpx 150, Hb 157

Graham and Powell		666 °C			
Kohn and Spear	at	550 °C	= 6.3 Kb	650 °C	= 7.5 Kb
(model 2 Mg)		600	= 6.9	700	= 8.0
Pattison and Newton	at	6.5 Kb	= 569 °C	7.5 Kb	= 575 °C
		7	= 572	8	= 578
Ellis and Green	at	6 Kb	= 692 °C	8 Kb	= 697 °C
		7	= 695	9	= 700

Gnt 160(core), Plag 152(matrix), Cpx 150, Hb157

Newton and Perkins	at	700 °C	= 7.4 Kb
Simultaneous Solution		696 °C,	7.4 Kb

'Embayed' Garnet - Rim
Gnt 162(rim), Plag 152(matrix), Cpx 150, Hb 157

Graham and Powell		610 °C			
Kohn and Spear	at	550 °C	= 6.3 Kb	650 °C	= 7.4 Kb
(model 2 Mg)		600	= 6.9	700	= 8.0
Pattison and Newton	at	5.5 Kb	= 482 °C	7 Kb	= 490 °C
		6	= 485	7.5	= 493
		6.5	= 488	8	= 496
Newton and Perkins	at	700 °C	= 6.0 Kb		
Simultaneous Solution		637 °C,	5.7 Kb		
Ellis and Green	at	5 Kb	= 635 °C	7 Kb	= 640 °C
		6	= 638	8	= 643

'Broken' Garnet - Core
Gnt 139(core on broken edge), Plag 140, Cpx 150

Newton and Perkins	at	700 °C	= 5.4 Kb		
Simultaneous Solution		640 °C,	5.1 Kb		
Ellis and Green	at	4 Kb	= 637 °C	6 Kb	= 643 °C
		5	= 640	7 Kb	= 645

Gnt 134(rim), Plag 140, Cpx 150

Newton and Perkins	at	700 °C	= 6.4 Kb		
Simultaneous Solution		679 °C,	6.3 Kb		
Ellis and Green	at	5 Kb	= 676 °C	7 Kb	= 681 °C
		6	= 679	8	= 684

APPENDIX IV

Geothermometry and Geobarometry Results

Sample R01f (continued)

'Regular' Garnet - Core
Gnt 79(core), Plag 152(matrix), Cpx 150

Newton and Perkins	at 700 °C	= 6.3 Kb			
Simultaneous Solution	643 °C,	5.9 Kb			
Ellis and Green	at 5 Kb	= 640 °C	7 Kb	= 645 °C	
	6	= 643	8	= 648	

'Regular' Garnet - Rim
Gnt 81(rim), Plag 152(matrix), Cpx 150

Newton and Perkins	at 700 °C	= 6.5 Kb			
Simultaneous Solution	688 °C,	6.4 Kb			
Ellis and Green	at 5 Kb	= 684 °C	7 Kb	= 689 °C	
	6	= 686	8	= 692	

Two-Way Zoned Garnet - Core
Gnt 175(core), Plag 152(matrix), Cpx 150

Newton and Perkins	at 700 °C	= 5.9 Kb			
Simultaneous Solution	623 °C,	5.5 Kb			
Ellis and Green	at 4 Kb	= 620 °C	6 Kb	= 625 °C	
	5	= 622	7	= 627	

Two-way Zoned Garnet - Interior
Gnt 174(interior), Plag 152(matrix), Cpx 150

Newton and Perkins	at 700 °C	= 6.5 Kb			
Simultaneous Solution	647 °C,	6.2 Kb			
Ellis and Green	at 5 Kb	= 644 °C	7 Kb	= 649 °C	
	6	= 646	8	= 651	

Two-Way Zoned Garnet - Rim
Gnt 173(rim), Plag 152(matrix), Cpx 150

Newton and Perkins	at 700 °C	= 6.5 Kb			
Simultaneous Solution	650 °C,	6.2 Kb			
Ellis and Green	at 5 Kb	= 647 °C	7 Kb	= 652 °C	
	6	= 649	8	= 654	

APPENDIX IV

Geothermometry and Geobarometry Results

Sample R07a

'Old' Garnet - Core
Gnt 7(core), Plag 13(core), Cpx 42(core), Hb 18

Graham and Powell		552 °C		
Kohn and Spear	at	550 °C	= 10.0 Kb	650 °C = 10.2 Kb
(Model 1 Mg)		600	= 10.1	700 = 10.3
Pattison and Newton	at	6 Kb	= 554 °C	8.5 Kb = 567 °C
		6.5	= 556	9 = 570
		7	= 559	9.5 = 573
		7.5	= 562	10 = 576
		8	= 565	
Newton and Perkins	at	700 °C	= 6.4 Kb	
Simultaneous Solution		565 °C,	6.1 Kb	
Ellis and Green	at	6 Kb	= 656 °C	9 Kb = 663 °C
		7	= 658	10 = 665
		8	= 661	

'Old' Garnet - Rim
Gnt 4(rim), Plag 12(rim), Cpx 41(rim), Hb 18

Graham and Powell		617 °C		
Kohn and Spear	at	600 °C	= 9.7 Kb	700 °C = 10.0 Kb
(Model 1 Mg)		650	= 9.9	
Pattison and Newton	at	6 Kb	= 617 °C	8.5 Kb = 631 °C
		6.5	= 620	9 = 634
		7	= 623	9.5 = 636
		7.5	= 625	10 = 639
		8	= 628	
Newton and Perkins	at	700 °C	= 6.8 Kb	
Simultaneous Solution		689 °C,	6.7 Kb	
Ellis and Green	at	6 Kb	= 687 °C	9 Kb = 695 °C
		7	= 690	10 = 697
		8	= 692	

APPENDIX IV

Geothermometry and Geobarometry Results

Sample R07a (continued)

'New' Garnet - Core
Gnt 23(core), Plag 29(core), Cpx 42(core), Hb 27

Graham and Powell	746 °C		
Kohn and Spear	at 700 °C	= 9.7 Kb	750 °C = 9.7 Kb
(Model 1 Mg)			
Pattison and Newton	at 6.5 Kb	= 669 °C	8.5 Kb = 680 °C
	7	= 672	9 = 683
	7.5	= 675	9.5 = 686
	8	= 678	
Newton and Perkins	at 700 °C	= 7.3 Kb	
Simultaneous Solution	710 °C,	7.4 Kb	
Ellis and Green	at 6 Kb	= 706 °C	8 Kb = 711 °C
	7	= 709	9 = 714

'New' Garnet - Rim
Gnt 25(core), Plag 28(rim), Cpx 41(rim), Hb 26

Graham and Powell	740 °C		
Kohn and Spear	at 650 °C	= 9.6 Kb	750 °C = 9.7 Kb
(Model 1 Mg)	700	= 9.6	
Pattison and Newton	at 6.5 Kb	= 624 °C	8.5 Kb = 635 °C
	7	= 627	9 = 638
	7.5	= 630	9.5 = 641
	8	= 632	10 = 643
Newton and Perkins	at 700 °C	= 6.8 Kb	
Simultaneous Solution	690 °C,	6.7 Kb	
Ellis and Green	at 6 Kb	= 688 °C	9 Kb = 696 °C
	7	= 690	10 = 698
	8	= 693	

APPENDIX IV

Geothermometry and Geobarometry Results

Sample R13

Gnt 109(core), Plag 196, Cpx 125(core), Hb 121

Graham and Powell	817 °C		
Kohn and Spear	at 500 °C = 9.8 Kb	700 °C = 10.4 Kb	
(Model 1 Fe)	550 = 9.9	750 = 10.5	
	600 = 10.1	800 = 10.7	
	650 = 10.2	850 = 10.8	
Pattison and Newton	at 6 Kb = 521 °C	8.5 Kb = 535 °C	
	6.5 = 524	9 = 537	
	7 = 526	9.5 = 540	
	7.5 = 529	10 = 543	
	8 = 532	10.5 = 546	
Newton and Perkins	at 700 °C = 6.3 Kb		
Simultaneous Solution	741 °C, 6.5 Kb		
Ellis and Green	at 6 Kb = 740 °C	9 Kb = 747 °C	
	7 = 742	10 = 750	
	8 = 745		

Gnt 107(rim), Plag 196, Cpx 128(rim), Hb 121

Graham and Powell	834 °C		
Kohn and Spear	at 500 °C = 9.9 Kb	700 °C = 10.6 Kb	
(Model 1 Fe)	550 = 10.1	750 = 10.7	
	600 = 10.2	800 = 10.9	
	650 = 10.4	850 = 11.0	
Pattison and Newton	at 6 Kb = 479 °C	9 Kb = 496 °C	
	6.5 = 482	9.5 = 499	
	7 = 485	10 = 501	
	7.5 = 488	10.5 = 504	
	8 = 490	11 = 507	
	8.5 = 493		
Newton and Perkins	at 700 °C = 6.4 Kb		
Simultaneous Solution	726 °C, 6.6 Kb		
Ellis and Green	at 6 Kb = 725 °C	9 Kb = 732 °C	
	7 = 727	10 = 735	
	8 = 730		

APPENDIX V

Electron Microprobe Analytical Methods

JEOL 733 Electron Microprobe

15 KV Excitation voltage
12 Nanoamps current
4 Wavelength spectrometer

LINK EDS (Energy Dispersive System)
Resolution of detector = 131 ev (electron volts on manganese).

Matrix correction program = LINK analytical ZAF program.

Spectra accumulated for 60 seconds.

Standards: Geological standards for garnet, plagioclase, clinopyroxene, hornblende, and biotite used as controls.

REFERENCES

Anovitz LM (1987) Pressure-temperature-time constraints on the metamorphism of the Grenville Province. Ph.D. thesis, University of Michigan, Ann Arbor. 479p.

Anovitz LM, Essene EJ (1986) Thermobarometry in the Grenville Province, Ontario. Geological Association of Canada, Program with abstracts 11:41.

Anovitz LM, Essene EJ (1990) Thermobarometry and pressure-temperature paths in the Grenville Province of Ontario. Journal of Petrology 31:197-241.

Baer AJ (1974) Grenville geology and plate tectonics. Geoscience Canada 1:54-61.

Barker AJ (1990) Introduction to Metamorphic Textures and Microstructures. Blackie and Son Ltd. New York. 170p.

Bégin NJ (1989) Metamorphic zonation, mineral chemistry and thermobarometry in metabasites of the Cape Smith Thrust-Fold Belt, northern Quebec: implications for its thermotectonic evolution. Ph.D. thesis, Queen's University, Kingston. 313p.

Culshaw NG, Check G, Corrigan D, Drage J, Gower R, Haggart MJ, Wallace P, Wodicka N (1989) Georgian Bay geological synthesis: Dillon to Twelve Mile Bay, Grenville Province of Ontario. In: Current Research, Part C, Geological Survey of Canada 89-1C:157-163.

Culshaw NG, Corrigan D, Drage J, Wallace P (1988) Georgian Bay geological synthesis: Key Harbour to Dillon, Grenville Province of Ontario. In: Current Research, Part C, Geological Survey of Canada 88-1C:129-133.

Culshaw NG, Corrigan D, Jamieson RA, Ketchum J, Wallace P, Wodicka N (1990b) Evidence for duplexing and extension in the ductile mid-crust from the Central Gneiss Belt, Grenville Province, Georgian Bay, Ontario. In: Thrust Tectonics 1990. McClay K (ed) Abstracts: 51.

Culshaw NG, Corrigan D, Jamieson RA, Ketchum J, Wallace P, Wodicka N (1991) Traverse of the Central Gneiss Belt, Grenville Province, Georgian Bay. Geological Association of Canada, Mineralogical Association of Canada, Society of Economic Geologists; Joint Annual Meeting, Toronto '91 Field Trip B3. Guidebook. 32p.

Culshaw NG, Corrigan D, Ketchum J, Wallace P (1990a) Georgian Bay geological synthesis: Twelve Mile Bay to Port Severn, Grenville Province of Ontario. In: Current Research, Part C Geological Survey of Canada 90-1C:107-112.

Culshaw NG, Davidson A, Nadeau L (1983) Structural subdivision of the Grenville Province in the Parry Sound Algonquin region, Ontario. In: Current Research, Part B, Geological Survey of Canada 83-1B:243-252.

Davidson A (1984) Identification of ductile shear zones in the southwestern Grenville Province of the Canadian Shield. In: Precambrian Tectonics Illustrated. Kroner A, Greiling R (eds) Schweizerbart'sche Verlagsbuchhandlung, Stuttgart: 263-279.

Davidson A (1990) Evidence for eclogite metamorphism in the southwestern Grenville Province. In: Current Research, Part C, Geological Survey of Canada 90-1C:113-118.

Davidson A (1991) Metamorphism and tectonic setting of gabbroic and related rocks in the Central Gneiss Belt, Grenville Province, Ontario. Geological Association of Canada, Mineralogical Association of Canada, Society of Economic Geologists; Joint Annual Meeting Toronto '91. Field Trip A2. Guidebook. 57p.

Davidson A, Bethune KM (1988) Geology of the north shore of Georgian Bay, Grenville Province of Ontario. In: Current Research, Part C, Geological Survey of Canada 88-1C:135-144.

Davidson A, Culshaw NG, Nadeau L (1982) A tectono-metamorphic framework for part of the Grenville Province, Parry Sound region, Ontario. In: Current Research, Part A, Geological Survey of Canada 82-1A:175-190.

Davidson A, Grant SM (1986) Reconnaissance geology of western and central Algonquin Park and detailed study of coronitic olivine metagabbro, Central Gneiss Belt, Grenville Province of Ontario. In: Current Research, Part B, Geological Survey of Canada 86-1B:837-848.

Davidson A, Morgan WC (1981) Preliminary notes on the geology east of Georgian Bay, Grenville Structural Province. In: Current Research, Part A, Geological Survey of Canada 81-1A:291-298.

Deer WA, Howie RA, Zussman J (1966) An Introduction to the Rock Forming Minerals. Longman Group Limited. Great Britain. 528p.

Ellis DJ, Green DH (1979) An experimental study of the effect of Ca upon garnet-clinopyroxene Fe-Mg exchange equilibria. Contributions to Mineralogy and Petrology 71:13-22.

Emslie RF, Hunt PA (1990) Ages and petrogenetic significance of igneous mangerite-charnockite suites associated with massive anorthosites, Grenville Province. Journal of Geology 98:213-231.

Essene EJ (1989) The current status of thermobarometry in metamorphic rocks. In: Evolution of Metamorphic Belts. Daly SJ, Cliff RA, Yardly BWD (eds). Geological Society Special Publication No.43:1-44.

Graham CM, Powell R (1984) A garnet-hornblende thermometer calibration, testing and application to the Pelona Schist, southern California. Journal of Metamorphic Geology 2:13-31.

Grant SM (1989) Tectonic implications from sapphirine-bearing lithologies, south-west Grenville Province, Canada. Journal of Metamorphic Geology 7:583-598.

Hanmer SK (1984) Structure of the junction of three tectonic slices; Ontario Gneiss Segment, Grenville Province. In: Current Research, Part B, Geological Survey of Canada 84-1B:109-120.

Hendriks M (1988) Garnet-hornblende geothermometer. Class assignment for Advanced Metamorphic Petrology, Dalhousie University. 3p.

Holdaway MJ (1971) Stability of andalusite and the aluminum silicate phase diagrams. American Journal of Science 271:97-131.

Jamieson RA (1988) Garnet-clinopyroxene geothermometry. Class assignment for Advanced Metamorphic Petrology, Dalhousie University. 3p.

Jamieson RA, Culshaw NG, Wodicka N, Corrigan D, Ketchum JWF (1992) Timing and tectonic setting of Grenvillian metamorphism - constraints from a transect along Georgian Bay, Ontario. Journal of Metamorphic Geology, special volume. Metamorphic styles in young and ancient orogenic belts. 10(3):321-332.

Ketchum JWF (1988) Garnet-plagioclase-pyroxene-quartz geobarometry. Class assignment for Advanced Metamorphic Petrology, Dalhousie University. 4p.

Kohn MJ, Spear FS (1989) Empirical calibration of geobarometers for the assemblage garnet + hornblende + plagioclase + quartz. American Mineralogist 74:77-84.

Leake BE, Winchell H (1978) Nomenclature of amphibols. American Mineralogist 63:1023-1052.

Mengel F, Rivers T (1991) Decompression reactions and P-T conditions in high grade rocks, northern Labrador: P-T-t paths from individual samples and implications for Early Proterozoic tectonic evolution. Journal of Petrology 32:139-167.

Moecher DP, Essene EJ (1990) Scapolite phase equilibria: additional constraints on the role of CO_2 in granulite genesis. In: Granulites and Crustal Evolution. Vielzeuf D., Vidal P. (eds.) Netherlands, Kluwer Academic Publishers: 385-396.

Nadeau L (1984) Deformation of Leucogabbro at Parry Sound, Ontario. M.Sc. thesis, Carleton University, Ottawa. 191p.

Needham TW (1987) Geological setting of two metagabbro bodies, central Britt domain, southwestern Grenville Province, Ontario. In: Current Research, Part A, Geological Survey of Canada 87-1A:597-603.

Newton RC, Perkins III D (1982) Thermodynamic calibration of geobarometers based on the assemblage garnet-plagioclase-orthopyroxene-(clinopyroxene)-quartz. American Mineralogist 67:203-222.

O'Beirne-Ryan AM, Jamieson RA, Gagnon YD (1989) Petrology of garnet-clinopyroxene amphibolites from Mont Albert, Gaspé, Quebec. Canadian Journal of Earth Sciences 27:72-86.

Pattison DRM (1991) Infiltration-driven dehydration and anatexis in granulite facies metagabbro, Grenville Province, Ontario, Canada. Journal of Metamorphic Geology 9:315-332.

Pattison DRM, Newton RC (1989) Revised experimental calibration of the garnet-clinopyroxene Fe-Mg exchange thermometer. Contributions to Mineralogy and Petrology 101:87-103.

Raase P (1974) Al and Ti contents of hornblende, indicators of pressure and temperature of regional metamorphism. Contributions to Mineralogy and Petrology 45:231-236.

Richard LR, Clarke DB (1990) AMPHIBOL: A program for calculating structural formulae and for classifying and plotting chemical analyses of amphiboles. American Mineralogist 75:421-423.

Rivers T, Martignole J, Gower CF, Davidson A (1989) New tectonic divisions of the Grenville Province, southeast Canadian Shield. Tectonics 8:63-84.

St-Onge MR, Lucas SB (1991) Evolution of regional metamorphism in the Cape Smith Thrust Belt (northern Quebec, Canada): interaction of tectonic and thermal processes. Journal of Metamorphic Geology 9:515-534.

Thompson AB, Rubie DC (eds) (1985) Metamorphic Reactions: Kinetics, Textures, and Deformation. Advances in Physical Geochemistry Volume 4. Springer-Verlag, New York, 291p.

Tracy RJ (1982) Compositional zoning and inclusions in metamorphic minerals. In: Characterization of Metamorphism through Mineral Equilibria. Mineralogical Society of America, Reviews in Mineralogy 10:355-397.

Tuccillo ME, Essene EJ, van der Pluijm BA (1990) Growth and retrograde zoning in garnets from high-grade metapelites: implications for pressure-temperature paths. Geology 18:839-842.

van Breemen O, Davidson A, Loveridge WD, Sullivan RW (1986) U-Pb zircon geochronology of Grenville tectonites, granulites and igneous precursors, Parry Sound, Ontario. In: The Grenville Province. Moore JM, Davidson A, Baer AJ (eds) Geological Association of Canada, Special Paper 31:191-207.

Wells PRA (1979) Chemical and thermal evolution of Archaean sialic crust, southern West Greenland. Journal of Petrology 20(2):187-226.

Wodicka N (1990) Geology and petrology of the Parry Sound domain, Grenville Province, Georgian Bay, Ontario: A proposal for research leading to the degree of Doctor of Philosophy, Dalhousie University, Halifax. 44p.

Wynne-Edwards HR (1972) The Grenville Province. In: Variations in Tectonic Styles in Canada. Price RA, Douglas RJW (eds) Geological Association of Canada Special Paper 11:263-334.

Yardley BWD (1989) An introduction to Metamorphic Petrology. Longman Scientific and Technical, Great Britain, 248p.